intensities were evaluated by relative build-up rates of the cross-peaks. Temperature dependence of the chemical shifts of all of the amide protons was investigated in **23c−e**, **23o**, and **23p**. In **23c**, the temperature coefficients for all of the NH protons were large. In **23d**, the only temperature coefficient for the NH of D-Tyr^3 was small, but NOE was not observed between the Nal^1 C$^\alpha$H and D-Tyr^3 NH. In **23e**, **23o**, and **23p**, the temperature coefficients for the NH of D-Tyr^3 and Arg^5 were small, but NOE was not observed between the Nal^1 C$^\alpha$H and D-Tyr^3 NH or between the D-Tyr^3 C$^\alpha$H and Arg^5 NH. Thus, no hydrogen bond restraints were used in the simulated annealing calculations of **23c−e**, **23o**, and **23p**.

Calculation of Structures. The structure calculations were performed on a Silicon Graphics Origin 2000 workstation with the NMR-refine program within the Insight II/Discover package using the consistent valence force field (CVFF).[55] Pseudoatoms were defined for the methylene protons of Nal^1, D-Tyr^3, Arg^4, and Arg^5 prochiralities of which were not identified by ^{1}H NMR data. The restraints, in which the Gly^2 α-methylene participated, were defined for the separate protons without definition of the prochiralities. The dihedral ϕ angle constraints were calculated based on the Karplus equation: $^3J(H^N,H^\alpha) = 6.7\cos^2(\theta - 60) - 1.3\cos(\theta - 60) + 1.5$.[56] Lower and upper angle errors were set to 15°. The NOESY spectrum with a mixing time of 400 ms was used for the estimation of the distance restraints between protons. The NOE intensities were classified into three categories (strong, medium, and weak) based on the number of contour lines in the cross-peaks to define the upper-limit distance restraints (2.7, 3.5, and 5.0 Å, respectively). The upper-limit restraints were increased by 1.0 Å for the involved pseudoatoms. Lower bounds between nonbonded atoms were set to their van der Waals radii (1.8 Å). These distance and dihedral angle restraints were included with force constants of 25−100 kcal/mol·Å^2 and 25−100 kcal/mol·rad^2, respectively. The 50 initial structures generated by the NMR refine program randomly were subjected to the simulated annealing calculations. The final minimization stage was achieved until the maximum derivative became less than 0.01 kcal/mol·Å^2 by the steepest descents and conjugate gradients methods.

Acknowledgment. This work was supported in part by a 21st Century COE Program "Knowledge Information Infrastructure for Genome Science", a Grant-in-Aid for Scientific Research from the Ministry of Education, Culture, Sports, Science and Technology, Japan, and the Japan Health Science Foundation. Computation time was provided by the Supercomputer Laboratory, Institute for Chemical Research, Kyoto University. S.U. is grateful for a Research Fellowship from the Japan Society for the Promotion of Science for Young Scientists.

Supporting Information Available: Characterization data of representative synthetic compounds and HPLC charts of **11a**, **11c**, **15e**, **16e**, **15q**, **16q**, **20a**, **20d**, **23d**, **23j**, **23o**, and **23p**. This material is available free of charge via the Internet at http://pubs.acs.org.

References

(1) Nagasawa, T.; Kikutani, H.; Kishimoto, T. Molecular cloning and structure of a pre-B-cell growth-stimulating factor. *Proc. Natl. Acad. Sci. U.S.A.* **1994**, *91*, 2305−2309.
(2) Bleul, C. C.; Farzan, M.; Choe, H.; Parolin, C.; Clark-Lewis, I.; Sodroski, J.; Springer, T. A. The lymphocyte chemoattractant SDF-1 is a ligand for LESTR/fusin and blocks HIV-1 entry. *Nature* **1996**, *382*, 829−833.
(3) Oberlin, E.; Amara, A.; Bachelerie, F.; Bessia, C.; Virelizier, J.-L.; Arenzana-Seisdedos, F.; Schwartz, O.; Heard, J.-M.; Clark-Lewis, I.; Legler, D. F.; Loetscher, M.; Baggiolini, M.; Moser, B. The CXC chemokine SDF-1 is the ligand for LESTR/fusin and prevents infection by T-cell-line-adapted HIV-1. *Nature* **1996**, *382*, 833−835.
(4) Tashiro, K.; Tada, H.; Heilker, R.; Shirozu, M.; Nakano, T.; Honjo, T. Signal sequence trap: a cloning strategy for secreted proteins and type I membrane proteins. *Science* **1993**, *261*, 600−603.
(5) Feng, Y.; Broder, C. C.; Kennedy, P. E.; Berger, E. A. HIV-1 entry co-factor: Functional cDNA cloning of a seven-transmembrane, G protein-coupled receptor. *Science* **1996**, *272*, 872−877.
(6) Müller, A.; Homey, B.; Soto, H.; Ge, N.; Catron, D.; Buchanan, M. E.; McClanahan, T.; Murphy, E.; Yuan, W.; Wagner, S. N.; Barrera, J. L.; Mohar, A.; Verastegui, E.; Zlotnik, A. Involvement of chemokine receptors in breast cancer metastasis. *Nature* **2001**, *410*, 50−56.
(7) Koshiba, T.; Hosotani, R.; Miyamoto, Y.; Ida, J.; Tsuji, S.; Nakamura, S.; Kawaguchi, M.; Kobayashi, H.; Doi, R.; Hori, T.; Fujii, N.; Imamura, M. Expression of stromal cell-derived factor 1 and CXCR4 ligand receptor system in pancreatic cancer: a possible role for tumor progression. *Clin. Cancer Res.* **2000**, *6*, 3530−3535.
(8) Mori, T.; Doi, R.; Koizumi, K.; Toyoda, E.; Tulachan, S. S.; Ito, D.; Kami, K.; Masui, T.; Fujimoto, K.; Tamamura, H.; Hiramatsu, K.; Fujii, N.; Imamura, M. CXCR4 antagonist inhibits stromal cell-derived factor 1-induced migration and invasion of human pancreatic cancer. *Mol. Cancer Ther.* **2004**, *3*, 29−37.
(9) Robledo, M. M.; Bartolome, R. A.; Longo, N.; Miguel Rodriguez-Frade, J.; Mellado, M.; Longo, I.; van Muijen, G. N. P.; Sanchez-Mateos, P.; Teixido, J. Expression of functional chemokine receptors CXCR3 and CXCR4 on human melanoma cells. *J. Biol. Chem.* **2001**, *276*, 45098−45105.
(10) Taichman, R. S.; Cooper, C.; Keller, E. T.; Pienta, K. J.; Taichman, N. S.; McCauley, L. K. Use of the stromal cell-derived factor-1/CXCR4 pathway in prostate cancer matastasis to bone. *Cancer Res.* **2002**, *62*, 1832−1837.
(11) Schrader, A. J.; Lechner, O.; Templin, M.; Dittmar, K. E. J.; Machtens, S.; Mengel, M.; Probst-Kepper, M.; Franzke, A.; Wollensak, T.; Gatzlaff, P.; Atzpodien, J.; Buer, J.; Lauber, J. CXCR4/CXCL12 expression and signalling in kidney cancer. *Br. J. Cancer* **2002**, *86*, 1250−1256.
(12) Geminder, H.; Sagi-Assif, O.; Goldberg, L.; Meshel, T.; Rechavi, G.; Witz, I. P.; Ben-Baruch, A. A possible role for CXCR4 and its ligand, the CXC chemokine stromal cell-derived factor-1, in the development of bone marrow metastases in neuroblastoma. *J. Immunol.* **2001**, *167*, 4747−4757.
(13) Bertolini, F.; Dell'Agnola, C.; Mancuso, P.; Rabascio, C.; Burlini, A.; Monestiroli, S.; Gobbi, A.; Pruneri, G.; Martinelli, G. CXCR4 neutralization, a novel therapeutic approach for non-Hodgkin's lymphoma. *Cancer Res.* **2002**, *62*, 3106−3112.
(14) Kijima, T.; Maulik, G.; Ma, P. C.; Tibaldi, E. V.; Turner, R. E.; Rollins, B.; Sattler, M.; Johnson, B. E.; Salgia, R. Regulation of cellular proliferation, cytoskeletal function, and signal transduction through CXCR4 and c-Kit in small cell lung cancer cells. *Cancer Res.* **2002**, *62*, 6304−6311.
(15) Scotton, C. J.; Wilson, J. L.; Milliken, D.; Stamp, G.; Balkwill, F. R. Epithelial cancer cell migration: a role for chemokine receptors? *Cancer Res.* **2001**, *61*, 4961−4965.
(16) Scotton, C. J.; Wilson, J. L.; Scott, K.; Stamp, G.; Wilbanks, G. D.; Fricker, S.; Bridger, G.; Balkwill, F. R. Multiple actions of the chemokine CXCL12 on epithelial tumor cells in human ovarian cancer. *Cancer Res.* **2002**, *62*, 5930−5938.
(17) Sanz-Rodriguez, F.; Hidalgo, A.; Teixido, J. Chemokine stromal cell-derived factor-1α modulates VLA-4 integrin-mediated multiple myeloma cell adhesion to CS-1/fibronectin and VCAM-1. *Blood* **2001**, *97*, 346−351.
(18) Tsukada, N.; Burger, J. A.; Zvaifler, N. J.; Kipps, T. J. Distinctive features of "nurselike" cells that differentiate in the context of chronic lymphocytic leukemia. *Blood* **2002**, *99*, 1030−1037.
(19) Juarez, J.; Bradstock, K. F.; Gottlieb, D. J.; Bendall, L. J. Effects of inhibitors of the chemokine receptor CXCR4 on acute lymphoblastic leukemia cells in vitro. *Leukemia* **2003**, *17*, 1294−1300.
(20) Rubin, J. B.; Kung, A. L.; Klein, R. S.; Chan, J. A.; Sun, Y.-P.; Schmidt, K.; Kieran, M. W.; Luster, A. D.; Segal, R. A. A small-molecule antagonist of CXCR4 inhibits intracranial growth of primary brain tumors. *Proc. Natl. Acad. Sci. U.S.A.* **2003**, *100*, 13513−13518.
(21) Nanki, T.; Hayashida, K.; El-Gabalawy, H. S.; Suson, S.; Shi, K.; Girschick, H. J.; Yavuz, S.; Lipsky, P. E. Stromal cell-derived factor-1-CXC chemokine receptor 4 interactions play a central role in CD4$^+$ T cell accumulation in rheumatoid arthritis synovium. *J. Immunol.* **2000**, *165*, 6590−6598.
(22) Tamamura, H.; Xu, Y.; Hattori, T.; Zhang, X.; Arakaki, R.; Kanbara, K.; Omagari, A.; Otaka, A.; Ibuka, T.; Yamamoto, N.; Nakashima, H.; Fujii, N. A low molecular weight inhibitor against the chemokine receptor CXCR4: a strong anti-HIV peptide T140. *Biochem. Biophys. Res. Commun.* **1998**, *253*, 877−882.
(23) Tamamura, H.; Hori, A.; Kanzaki, N.; Hiramatsu, K.; Mizumoto, M.; Nakashima, H.; Yamamoto, N.; Otaka, A.; Fujii, N. T140 analogs as CXCR4 antagonists identified as anti-metastatic agents in the treatment of breast cancer. *FEBS Lett.* **2003**, *550*, 79−83.

(24) Tamamura, H.; Fujisawa, M.; Hiramatsu, K.; Mizumoto, M.; Nakashima, H.; Yamamoto, N.; Otaka, A.; Fujii, N. Identification of a CXCR4 antagonist, a T140 analog, as an anti-rheumatoid arthritis agent. *FEBS Lett.* **2004**, *569*, 99−104.
(25) Tamamura, H.; Omagari, A.; Oishi, S.; Kanamoto, T.; Yamamoto, N.; Peiper, S. C.; Nakashima, H.; Otaka, A.; Fujii, N. Pharmacophore identification of a specific CXCR4 inhibitor, T140, leads to development of effective anti-HIV agents with very high selectivity indexes. *Bioorg. Med. Chem. Lett.* **2000**, *10*, 2633−2637.
(26) Fujii, N.; Oishi, S.; Hiramatsu, K.; Araki, T.; Ueda, S.; Tamamura, H.; Otaka, A.; Kusano, S.; Terakubo, S.; Nakashima, H.; Broach, J. A.; Trent, J. O.; Wang, Z.; Peiper, S. C. Molecular-size reduction of a potent CXCR4-chemokine antagonist using orthogonal combination of conformation- and sequence-based libraries. *Angew. Chem., Int. Ed.* **2003**, *42*, 3251−3253.
(27) Fukami, T.; Nagase, T.; Fujita, K.; Hayama, T.; Niiyama, K.; Mase, T.; Nakajima, S.; Fukuroda, T.; Saeki, T.; Nishikibe, M.; Ihara, M.; Yano, M.; Ishikawa, K. Structure−activity relationships of cyclic pentapeptide endothelin A receptor antagonists. *J. Med. Chem.* **1995**, *38*, 4309−4324.
(28) Haubner, R.; Gratias, R.; Diefenbach, B.; Goodman, S. L.; Jonczyk, A.; Kessler, H. Structural and functional aspects of RGD-containing cyclic pentapeptides as highly potent and selective integrin $\alpha V\beta 3$ antagonists. *J. Am. Chem. Soc.* **1996**, *118*, 7461−7472.
(29) Spatola, A. F.; Crozet, Y.; deWit, D.; Yanagisawa, M. Rediscovering an endothelin antagonist (BQ-123): A self-deconvoluting cyclic pentapeptide library. *J. Med. Chem.* **1996**, *39*, 3842−3846.
(30) Wermuth, J.; Goodman, S. L.; Jonczyk, A.; Kessler, H. Stereoisomerism and biological activity of the selective and superactive $\alpha V\beta 3$ integrin inhibitor cyclo(−RGDfV-) and its retro-inverso peptide. *J. Am. Chem. Soc.* **1997**, *119*, 1328−1335.
(31) Haubner, R.; Finsinger, D.; Kessler, H. Stereoisomeric peptide libraries and peptidomimetics for designing selective inhibitors of the $\alpha V\beta 3$ integrin for a new cancer therapy. *Angew. Chem., Int. Ed. Engl.* **1997**, *36*, 1374−1389.
(32) Porcelli, M.; Casu, M.; Lai, A.; Saba, G.; Pinori, M.; Cappelletti, S.; Mascagni, P. Cyclic pentapeptides of chiral sequence DLDDL as scaffold for antagonism of G-protein coupled receptors: Synthesis, activity and conformational analysis by NMR and molecular dynamics of ITF 1565 a substance P inhibitor. *Biopolymers* **1999**, *50*, 211−219.
(33) Oishi, S.; Kamano, T.; Niida, A.; Odagaki, Y.; Hamanaka, N.; Yamamoto, M.; Ajito, K.; Tamamura, H.; Otaka, A.; Fujii, N. Diastereoselective synthesis of new ψ[[(*E*)-CH=CMe]- and ψ-[[(*Z*)-CH=CMe]-type alkene dipeptide isosteres by organocopper reagents and application to conformationally restricted cyclic RGD peptidomimetics. *J. Org. Chem.* **2002**, *67*, 6162−6173.
(34) Nikiforovich, G. V.; Kover, K. E.; Zhang, W.-J.; Marshall, G. R. Cyclopentapeptides as flexible conformational templates. *J. Am. Chem. Soc.* **2000**, *122*, 3262−3273.
(35) Tamamura, H.; Hiramatsu, K.; Ueda, S.; Wang, Z.; Kusano, S.; Terakubo, S.; Trent, J. O.; Peiper, S. C.; Yamamoto, N.; Nakashima, H.; Otaka, A.; Fujii, N. Stereoselective synthesis of [L-Arg-L/D-3-(2-naphthyl)alanine]-type (*E*)-alkene dipeptide isosteres and its application to the synthesis and biological evaluation of pseudopeptide analogues of the CXCR4 antagonist FC131. *J. Med. Chem.* **2005**, *48*, 380−391.
(36) Abdel-Magid, A. F.; Maryanoff, C. A.; Carson, K. G. Reductive amination of aldehydes and ketones by using sodium triacetoxyborohydride. *Tetrahedron Lett.* **1990**, *31*, 5595−5598.
(37) Fukuyama, T.; Jow, C.-K.; Cheung, M. 2- and 4-Nitrobenzenesulfonamides: exceptionally versatile means for preparation of secondary amines and protection of amines. *Tetrahedron Lett.* **1995**, *36*, 6373−6374.
(38) Myers, A. G.; Gleason, J. L.; Yoon, T.; Kung, D. W. Highly practical methodology for the synthesis of D- and L-*R*-amino acids, N-protected *R*-amino acids, and *N*-methyl-*R*-amino acids. *J. Am. Chem. Soc.* **1997**, *119*, 656−673.
(39) Travins, J. M.; Etzkorn, F. A. Facile synthesis of D-amino acids from an L-serine-derived aziridine. *Tetrahedron Lett.* **1998**, *39*, 9389−9392.
(40) Biagini, S. C. G.; Gibson, S. E.; Keen, S. P. Cross-metathesis of unsaturated α-amino acid derivatives. *J. Chem. Soc., Perkin. Trans. 1* **1998**, 2485−2499.
(41) Oppolzer, W.; Lienard, P. Non-destructive cleavage of *N*-acylsultams under neutral conditions: preparation of enantiomerically pure, Fmoc-protected α-amino acids. *Helv. Chim. Acta* **1992**, *75*, 2572−2582.
(42) Douat, C.; Heitz, A.; Martinez, J.; Fehrentz, J.-A. Stereoselective synthesis of allyl- and homoallylglycines. *Tetrahedron Lett.* **2001**, *42*, 3319−3321.
(43) Scholl, M.; Ding, S.; Lee, C. W.; Grubbs, R. H. Synthesis and activity of a new generation of ruthenium-based olefin metathesis catalysts coordinated with 1,3-dimesityl-4,5-dihydroimidazol-2-ylidene ligands. *Org. Lett.* **1999**, *1*, 953−956.
(44) Tamaki, M.; Han, G.; Hruby, V. J. Practical and efficient synthesis of orthogonally protected constrained 4-guanidinoprolines. *J. Org. Chem.* **2001**, *66*, 1038−1042.
(45) Tamamura, H.; Sugioka, M.; Odagaki, Y.; Omagari, A.; Kan, Y.; Oishi, S.; Nakashima, H.; Yamamoto, N.; Peiper, S. C.; Hamanaka, N.; Otaka, A.; Fujii, N. Conformational study of a highly specific CXCR4 inhibitor, T140, disclosing the close proximity of its intrinsic pharmacophores associated with strong anti-HIV activity. *Bioorg. Med. Chem. Lett.* **2001**, *11*, 359−362 and 2409.
(46) Intramolecular hydrogen bonds were not observed in the calculated structures of these cyclic pentapeptides. Thus, these peptides do not seem to exist in a characteristic turn conformation such as a βII′γ turn as reported in several papers concerning normal cyclic pentapeptides, see Weisshoff, H.; Prasang, C.; Henklein, P.; Frommel, C.; Zschunke, A.; Mugge, C. Mimicry of βII′-turns of proteins in cyclic pentapeptides with one and without D-amino acids. *Eur. J. Biochem.* **1999**, *259*, 776−788.
(47) Murakami, T.; Nakajima, T.; Koyanagi, Y.; Tachibana, K.; Fujii, N.; Tamamura, H.; Yoshida, N.; Waki, M.; Matsumoto, A.; Yoshie, O.; Kishimoto, T.; Yamamoto, N.; Nagasawa, T. A small molecule CXCR4 inhibitor that blocks T cell line-tropic HIV-1 infection. *J. Exp. Med.* **1997**, *186*, 1389−1393.
(48) Schols, D.; Struyf, S.; Van Damme, J.; Este, J. A.; Henson, G.; De Clercq, E. Inhibition of T-tropic HIV strains by selective antagonization of the chemokine receptor CXCR4. *J. Exp. Med.* **1997**, *186*, 1383−1388.
(49) Donzella, G. A.; Schols, D.; Lin, S. W.; Este J. A.; Nagashima, K. A.; Maddon, P. J.; Allaway, G. P.; Sakmar, T. P.; Henson, G.; De Clercq, E.; Moore, J. P. AMD3100, a small molecule inhibitor of HIV-1 entry via the CXCR4 co-receptor. *Nat. Med.* **1998**, *4*, 72−77.
(50) Doranz, B. J.; Grovit-Ferbas, K.; Sharron, M. P.; Mao, S.-H.; Bidwell Goetz, M.; Daar, E. S.; Doms, R. W.; O'Brien, W. A. A small-molecule inhibitor directed against the chemokine receptor CXCR4 prevents its use as an HIV-1 coreceptor. *J. Exp. Med.* **1997**, *186*, 1395−1400.
(51) Howard, O. M. Z.; Oppenheim, J. J.; Hollingshead, M. G.; Covey, J. M.; Bigelow, J.; McCormack, J. J.; Buckheit, Jr., R. W.; Clanton, D. J.; Turpin, J. A.; Rice, W. G. Inhibition of in vitro and in vivo HIV replication by a distamycin analogue that interferes with chemokine receptor function: a candidate for chemotherapeutic and microbicidal application. *J. Med. Chem.* **1998**, *41*, 2184−2193.
(52) Fujii, N.; Nakashima, H.; Tamamura, H. The Therapeutic Potential of CXCR4 Antagonists in the Treatment of HIV. *Expert Opin. Investig. Drugs* **2003**, *12*, 185−195.
(53) Tamamura, H.; Fujii, N. Two Orthogonal Approaches to Overcome Multi-Drug Resistant HIV-1s: Development of Protease Inhibitors and Entry Inhibitors Based on CXCR4 Antagonists. *Curr. Drug Targets-Infect. Disord.* **2004**, *4*, 103−110.
(54) Navenot, J. M.; Wang , Z. X.; Trent, J. O.; Murray, J. L.; Hu, Q. X.; DeLeeuw, L.; Moore, P. S.; Chang, Y.; Peiper, S. C. Molecular anatomy of CCR5 engagement by physiologic and viral chemokines and HIV-1 envelope glycoproteins: Differences in primary structural requirements for RANTES, MIP-1α, and vMIP−II binding. *J. Mol. Biol.* **2001**, *313*, 1181−1193.
(55) Miyamoto, K.; Nakagawa, T.; Kuroda, Y. Solution structure of the cytoplasmic linker between domain III−S6 and domain IV−S1 (III−IV linker) of the rat brain sodium channel in SDS micelles. *Biopolymers* **2001**, *59*, 380−393.
(56) Ludvigsen, S.; Andersen, K. V.; Poulsen, F. M. Accurate measurements of coupling-constants from 2-dimensional nuclear-magnetic-resonance spectra of proteins and determination of ϕ-angles *J. Mol. Biol.* **1991**, *217*, 731−736.

JM050009H

Oncogene (2005) 24, 4462–4471

www.nature.com/onc

CXCR4 chemokine receptor and integrin signaling co-operate in mediating adhesion and chemoresistance in small cell lung cancer (SCLC) cells

Tanja N Hartmann[1], Jan A Burger[1], Aleksandra Glodek[2], Nobutaka Fujii[3] and Meike Burger*[,1]

[1]*Department of Medicine, Division of Hematology/Oncology, Freiburg University Hospital, Hugstetterstr. 55, D-79106 Freiburg, Germany;* [2]*Dana-Farber Cancer Institute, Harvard Medical School, Boston, USA;* [3]*Graduate School of Pharmaceutical Sciences, Kyoto University, Kyoto, Japan*

Small cell lung cancer (SCLC) is an aggressive, rapidly metastazising neoplasm with a high propensity for marrow involvement. SCLC cells express high levels of functional CXCR4 receptors for the chemokine stromal-cell-derived factor-1 (SDF-1/CXCL12). Adhesion of SCLC cells to extracellular matrix or accessory cells within the tumor microenvironment confers resistance to chemotherapy via integrin signaling and thus may be responsible for residual disease and relapses commonly seen in SCLC. We examined the signaling mechanisms that regulate CXCL12-induced adhesion of SCLC cells to fibronectin, collagen, and stromal cells and the effects on SCLC cell chemoresistance. We found that CXCL12-induced integrin activation which resulted in an increased adhesion of SCLC cells to fibronectin and collagen. This was mediated by α2, α4, α5, and β1 integrins along with CXCR4 activation, which could be inhibited by CXCR4 antagonists. Stromal cells protected SCLC cells from chemotherapy-induced apoptosis, and this protection could also be antagonized by CXCR4 inhibitors. We conclude that activation of integrins and CXCR4 chemokine receptors co-operate in mediating adhesion and survival signals from the tumor microenvironment to SCLC cells. Therefore, CXCR4 antagonists in combination with cytotoxic drugs should be explored in SCLC to overcome CXCL12-mediated adhesion and survival signals in the tumor microenvironment.
Oncogene (2005) **24,** 4462–4471. doi:10.1038/sj.onc.1208621
Published online 4 April 2005

Keywords: chemokine receptor; CXCR4; CXCR4 antagonists; integrins; lung cancer

Introduction

Small cell lung cancer (SCLC) is a particularly aggressive form of lung cancer. The early and widespread metastasis and the ability to develop resistance against chemotherapeutic drugs (Ihde, 1992; Hoffman *et al.*, 2000) are responsible for the highly malignant phenotype of SCLC. SCLC has a striking tendency to metastasize in the bone marrow (Lassen *et al.*, 1995). Metastasis of cancer cells involve the passage through the blood and/or lymphatic circulation and movement across vascular barriers. It is believed that metastatic cancer cells co-opt signals that normally control leukocyte trafficking, such as chemokine-mediated cell migration. According to the multistep paradigm of leukocyte migration, emigration from the vasculature and tissue homing is regulated by a sequence of distinct molecular signals (Springer, 1994). One key step of this sequence involves chemokines that activate integrins and direct the migration of leukocytes.

The chemokine stromal-cell-derived factor-1 (SDF-1/CXCL12) is a CXC chemokine constitutively expressed by marrow stromal cells. CXCR4, the sole CXCL12 receptor, plays a pivotal role for the homing of hematopoietic stem cells within the marrow microenvironment. There is growing evidence that the CXCR4/CXCL12 axis regulates migration and metastasis of a variety of cancers (Burger *et al.*, 1999; Geminder *et al.*, 2001; Muller *et al.*, 2001; Robledo *et al.*, 2001; Taichman *et al.*, 2002). *In vivo* neutralization of the CXCR4/CXCL12 axis resulted in inhibition or attenuation of metastases of breast cancer and NSCLC (Muller *et al.*, 2001; Phillips *et al.*, 2003). Because SCLC has a striking tendency to metastazise to the bone marrow (Hoffman *et al.*, 2000) and marrow stromal cells secrete high amounts of CXCL12, we hypothesize that the CXCR4/CXCL12 interaction is also involved in SCLC metastasis and protection from apoptosis in the tumor microenvironment.

CXCR4 engagement by CXCL12 leads to diverse biological responses, some of which are cell-type dependent. Binding of CXCL12 to CXCR4 induces activation of Gαi proteins, the phosphatidylinositol 3-kinase (PI3K) and mitogen-activated protein (MAP) kinase pathways in a range of cell types, including tumor cells like SCLC (Ganju *et al.*, 1998; Vicente-Manzanares *et al.*, 1998; Kijima *et al.*, 2002; Burger *et al.*, 2003b). CXCL12 can activate integrins and initiate firm adhesion of rolling leukocytes (Campbell *et al.*, 1998; Constantin *et al.*, 2000). It is suggested that CXCR4/CXCL12 interaction mediates cytoskeletal changes, since stimulation of CXCR4 transfectants by CXCL12

*Correspondence: M Burger; E-mail: burgerm@mm11.ukl.uni-freiburg.de
Received 28 September 2004; revised 8 February 2005; accepted 8 February 2005; published online 4 April 2005

resulted in increased phosphorylation of focal adhesion components, including the related adhesion focal tyrosine kinase (RAFTK/Pyk2), Crk and paxillin (Ganju *et al.*, 1998).

The integrins are a family of cell adhesion receptors that mediate the binding and responses of cells to extracellular matrix (ECM). They are involved in cell–ECM as well as in cell–cell interactions. Sethi *et al.* (1999) demonstrated that, *in vivo*, SCLC cells exist in an ECM-rich environment at both primary and secondary metastatic sites. The ECM stroma, which surrounds SCLC cells, contains fibronectin, laminin, collagen IV and tenascin. On the other side, SCLC cells express various α- and β-integrin chains that allow for interactions with the ECM containing tumor microenvironment. Correspondingly, adhesion of SCLC cells to ECM enhanced tumorigenicity of SCLC cells, induced a β1-integrin-stimulated tyrosine kinase activation, and resistance to chemotherapeutic agents (Sethi *et al.*, 1999). Recently we demonstrated that CXCL12 enhanced the adhesion of SCLC cells to immobilized VCAM-1, demonstrating that CXCR4 receptors can induce integrin activation on SCLC cells (Burger *et al.*, 2003b). In addition, CXCR4/CXCL12 interaction induced actin polymerization and firm adhesion of SCLC cells to marrow stromal cells, suggesting that this interaction may be involved in adhesive and migratory events in the bone marrow metastasis of SCLC cells.

In this study we further investigated the interaction between the CXCR4 signaling and the protective effect of β1-integrin engagement in SCLC cells. We demonstrate that SCLC cell adhesion to β1-integrin ligands fibronectin and collagen is increased by CXCL12. Rho GTPases are involved in the CXCL12-induced adhesion of SCLC cells and the focal-adhesion adaptor protein paxillin is activated by CXCL12 in NCI-H82 and NCI-N592 cells. Locking integrins in activated state by Manganese as well as coimmobilized CXCL12 partially reduces the chemosensitivity of SCLC cells. Moreover, we demonstrate that adhesion of SCLC cells to marrow stromal cells protects them from etoposide-induced apoptosis, which can be antagonized by CXCR4-specific antagonists and antibodies against α4 integrins.

Results

CXCL12 enhances adhesion to fibronectin and collagen

Previously we demonstrated that CXCL12 enhanced the adhesion of SCLC cells to immobilized VCAM-1, demonstrating that CXCR4 chemokine receptors can induce VLA-4 activation on SCLC cells. Sethi *et al.* (1999) showed that the adherence of SCLC cells to ECM proteins fibronectin and collagen protected the SCLC cells from chemotherapy-induced apoptosis. Adhesion assays were performed to test whether the SCLC cell adhesion to fibronectin and collagen is mediated by CXCR4/CXCL12 interaction. Using three different common SCLC cell lines we found that a part of the SCLC cells became adherent to fibronectin without stimulation. The percentage of cells being adherent without further stimulus differed from cell line to cell line, NCI-N592 cells showed the highest background adhesion to fibronectin. The adherence to fibronectin was significantly enhanced by coimmobilized CXCL12 in all tested cell lines (Figure 1a). To rule out unspecific adhesion, control wells were precoated with BSA instead of fibronectin or collagen. No adherent SCLC cells were detected in this case (data not shown), indicating that adhesion was dependent on fibronectin or collagen. Whereas all three SCLC cell lines showed background adhesion to fibronectin, only SCLC cell line NCI-N592 showed background adhesion to collagen. We observed a very robust activation of adhesion to collagen by coimmobilized CXCL12 in all three tested cell lines (Figure 1b).

α2-, α4- and α5-, as well as β1-integrin subunits are involved in the CXCL12-induced adhesion to fibronectin and collagen. We found high expression of integrin subunits α4 and α5 as well as β1 in SCLC cells (Figure 2). NCI-N592 also expressed α2-integrin subunits (Figure 2b). α3 expression was usually low; and α1 and β7 expression was absent in SCLC cells. Accordingly, CXCL12-induced adhesion of NCI-H82 cells to fibronectin could be inhibited with α4 as well as α5 blocking antibodies (Figure 1c). CXCL12-induced adhesion of NCI-H69 and NCI-N592 cells to collagen could be inhibited with α2 blocking antibodies but not with α1 or α3 blocking antibodies (Figure 1d). Isotype controls of the antibodies did not block adhesion to fibronectin or collagen.

Furthermore we tested if the CXCL12-induced adhesion to fibronectin and collagen could be inhibited with CXCR4 antagonist T140 and PT (Figure 1e and f). Whereas T140 significantly inhibited the CXCL12-induced adhesion, PT showed no inhibition, indicating that the CXCL12-induced adhesion to fibronectin is not Gαi mediated. In summary, our data indicate that the adhesion of SCLC cells to ECM components is mediated by CXCR4/CXCL12 interaction.

Rho kinase is involved in CXCL12 modulation of VLA-4-mediated SCLC cell adhesion

CXCL12 activates p44/42 MAP kinase as well as PI3 kinase in SCLC cells (Kijima *et al.*, 2002; Burger *et al.*, 2003b). We tested whether these pathways are necessary for the CXCL12-induced cell adhesion (Figure 3). Additionally, we tested whether src kinases are necessary for the CXCL12-induced adhesion. There was no inhibition of adhesion by PD98059, LY294002 and src kinase inhibitors PP1 and PP2 (data not shown). However, adhesion could be inhibited with Rho kinase inhibitor Y27632 and Toxin B, an inhibitor for the small Rho GTPases Rho, Rac and Cdc42. This suggests that Rho GTPases are involved in mediating CXCL12-induced adhesion of SCLC cells to VCAM-1 (Figure 3).

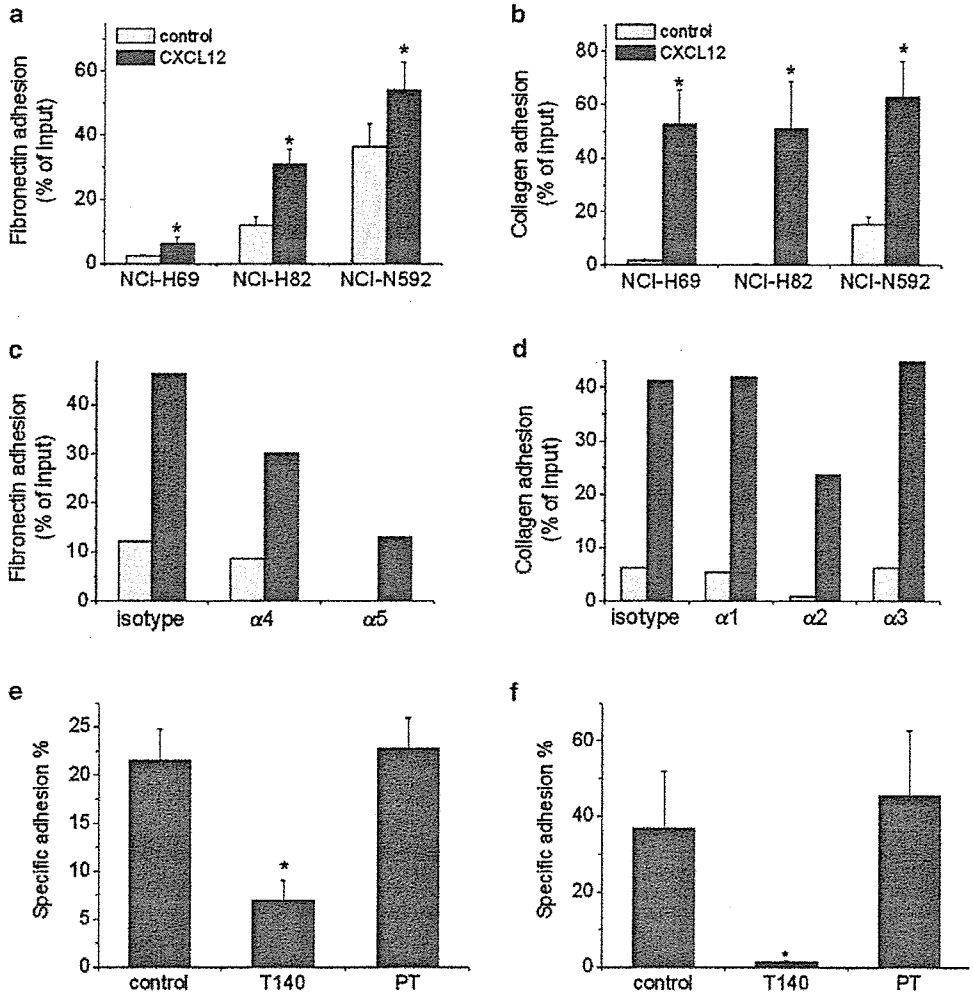

Figure 1 CXCL12 modulates adhesion to fibronectin and collagen. (**a**) SCLC cell adhesion to immobilized fibronectin is enhanced by CXCL12. Cells were allowed to adhere 30 min to fibronectin coated wells (10 μg/ml). Adhesions were quantified using CyQuant Cell Proliferation Kit. Coimmobilized CXCL12 (8 μg/ml) induced a significant increase in SCLC cell adhesion to fibronectin in SCLC cell lines NCI-H69, NCI-H82 and NCI-N592, as indicated by the asterisks depicted above the bars with $P \leqslant 0.05$. The black bars represent the relative proportion of adhering SCLC cells in comparison to SCLC cell adhesion to fibronectin without CXCL12 (gray bars). Adhesion data represent the mean and s.e.m. of at least five independent experiments, measured in quatriplicate samples. (**b**) SCLC cell adhesion to immobilized collagen I is enhanced by CXCL12. Cells were allowed to adhere 30 min to collagen coated wells (5 μg/ml). Adhesions were quantified using CyQuant Cell Proliferation Kit. Coimmobilized CXCL12 (8 μg/ml) induced a significant increase in SCLC cell adhesion to collagen I ($P \leqslant 0.05$). Adhesion data represent the mean and s.e.m. of at least five independent experiments, measured in quatriplicate samples. (**c**) CXCL12-mediated adhesion to fibronectin is $\alpha 4$ and $\alpha 5$ integrin dependent. NCI-H82 cells were preincubated with 5 μg/ml $\alpha 4$ and $\alpha 5$ blocking antibodies and the corresponding isotype control. One of two independent experiments, measured in quatriplicate, is shown. (**d**) CXCL12-mediated adhesion to collagen is $\alpha 2$, but not $\alpha 1$ or $\alpha 3$ dependent. NCI-N592 cells were preincubated with 20 μg/ml $\alpha 1$, $\alpha 2$, and $\alpha 3$ blocking antibodies and the corresponding isotype control. One of two independent experiments, measured in quatriplicate, is shown. (**e**) CXCL12-mediated adhesion of SCLC cells onto fibronectin is CXCR4, but not Gαi dependent. NCI-H82 cells were preincubated with CXCR4 antagonist T140 (300 μg/ml) and PT (500 ng/ml), an inhibitor of Gαi proteins. Inhibition of CXCR4 but not of Gai decreased the adhesion to fibronectin, suggesting that Gαi proteins are not involved in CXCR4-mediated $\beta 1$-integrin activation. Results are shown as specific adhesion (background adhesion in the absence of a stimulus was subtracted from CXCL12-induced adhesion). The experiment was performed three times in quatriplicate each and mean values $\pm$ standard errors are shown. (**f**) CXCL12-mediated adhesion of SCLC cells onto collagen is CXCR4, but not Gαi dependent. NCI-H82 cells were preincubated with T140 and PT as described in (e). Mean values $\pm$ standard errors from three independent experiments are shown

Tyrosine phosphorylation of components of focal adhesion complexes

Focal adhesions that contain part of the cytoskeleton and plasma membrane are structures that mediate adherent contacts with the ECM. The focal adhesion kinase (FAK) is thought to play an important role in cell adhesion and migration (Schaller, 2001), and the focal adhesion components paxillin and CrkL are thought to play important roles in chemotactic signaling pathways (Ganju *et al.*, 1998). Therefore we assessed FAK, paxillin and CrkL phosphorylation upon CXCL12 stimulation in SCLC cell lines NCI-H69, NCI-H82 and NCI-N592. All three cell lines tested showed

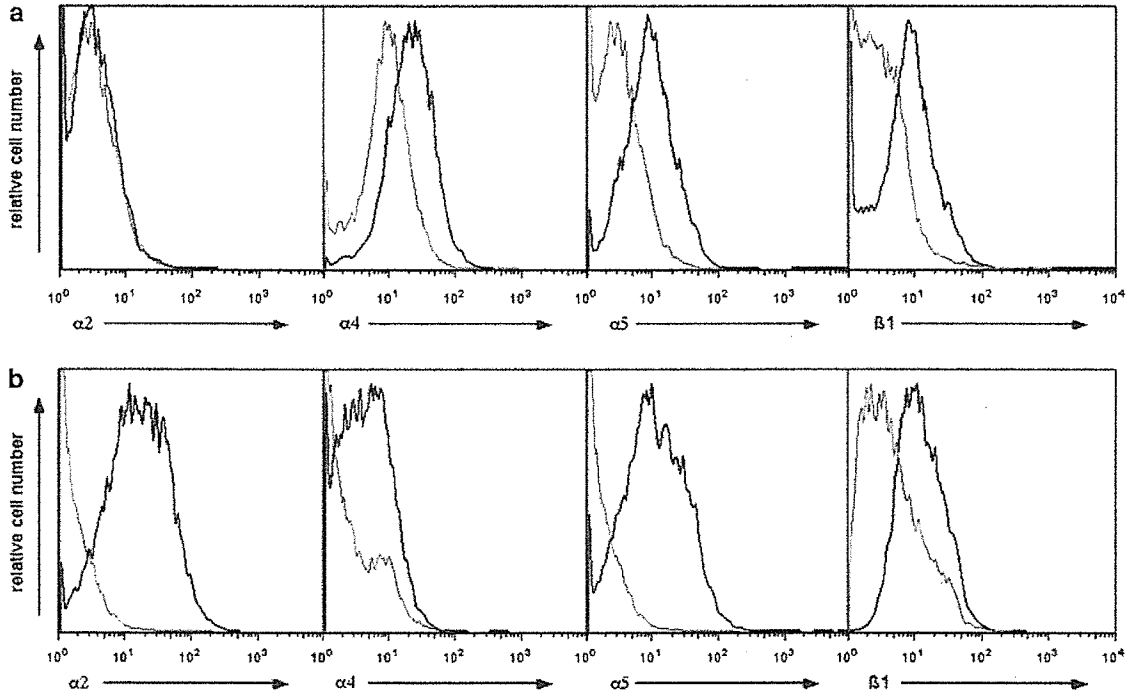

Figure 2 Expression of integrin subunits in SCLC cells. Logarithmic fluorescence histograms depicting the expression of $\alpha 2$ (CD49b), $\alpha 4$ (CD49d), $\alpha 5$ (CD49e) and $\beta 1$ (CD29)-integrin subunits in (**a**) NCI-H82 and (**b**) NCI-N592 cells. The black lines represent the staining for the specific monoclonal antibodies, while the grey lines show the isotype staining of the respective sample

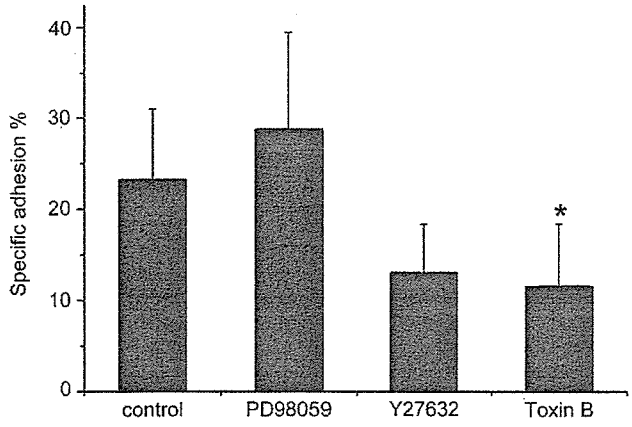

Figure 3 Pathways involved in CXCL12 modulation of VLA-4-mediated SCLC cell adhesion. CXCL12-mediated adhesion of SCLC cells is Rho dependent. NCI-N592 cells were preincubated with 20 μM PD98059, 10 μM Y27632 and 100 ng/ml Toxin B. Cells were allowed to adhere 30 min to VCAM-1 (1.3 μg/ml) and CXCL12 (8 μg/ml) coated wells. Adhesions were quantified using CyQuant Cell Proliferation Kit. Results are shown as specific adhesion (background adhesion in the absence of a stimulus was subtracted from CXCL12-induced adhesion). The experiment was performed four times in quatriplicate each and mean values $\pm$ standard errors are shown. The asterisk indicates significant differences to the control with $P \leqslant 0.05$

constitutive phosphorylation of FAK and CrkL which was unaffected by CXCL12 treatment. Figure 4a and b display time courses of constitutive FAK and CrkL phosphorylation of NCI-H82 representative for all three investigated cell lines. Densitometrical measurements of the blots confirmed the constitutive phosphorylation (data not shown).

The expression of paxillin is usually very low or nonexistent in SCLC samples (Salgia *et al.*, 1999). In NCI-H69 phosphorylated paxillin was undetectable, but in NCI-H82 and NCI-N592 cells, paxillin phosphorylation increased about 50% upon CXCL12 stimulation (Figure 4c), as confirmed by densitometrical measurements of the blots.

Soluble CXCL12 (sCXCL12) does not have direct proliferative or protective effects on SCLC cells

It has been suggested that CXCL12 may have a proliferative effect on SCLC cells (Kijima *et al.*, 2002). We performed several experiments to reveal a possible proliferative or antiapoptotic effect of CXCL12 on SCLC cells. First, cell proliferation was evaluated 48 h after stimulation by CXCL12 using the colorimetric MTT assay. Up to 500 ng/ml CXCL12 had no effect on proliferation of NCI-H69, NCI-H82 and NCI-N592 cells (data not shown). Second, apoptosis was induced by culturing SCLC cells in serum-free medium, and SCLC cell viability was cytometrically determined with $DIOC_6$/PI after 48 h, to test if there is an antiapoptotic effect of CXCL12. We found that the addition of sCXCL12 to media did not improve the survival of serum-starved cells (data not shown). Third, we cultivated NCI-H82 and NCI-N592 cells in full medium or serum-free medium and treated them with 100 or 200 μg/ml etoposide for 48 h to induce apoptosis

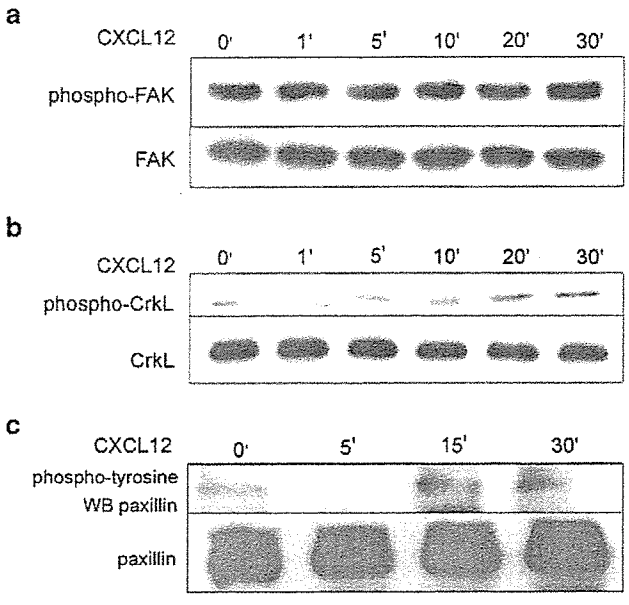

Figure 4 Tyrosine phosphorylation of components of focal adhesion complexes. (a, b) NCI-H82 cells were serum deprived and incubated with 100 ng/ml CXCL12 and cell lysates of equal amounts of cells were prepared at the indicated time points. Cell lysates were analysed by phospho-specific antibodies against FAK or CrkL. The bottom panels show the total protein detected by probing the blots with anti-FAK and anti-CrkL. The blots were performed at least three times on three different cells lines (NCI-H69, NCI-H82, NCI-N592) and a representative blot is shown. (c) For detection of phosphorylated paxillin, immunoprecipitations (IP) with phospho-tyrosine antibodies were performed using lysates prepared from NCI-N592 cells. The immune complexes were resolved on SDS–PAGE and Western blotted (WB) with paxillin antibody. The bottom panel shows total paxillin in the corresponding samples. The blots were done at least five times and a representative one is shown

(Figure 5). Addition of sCXCL12 to media could in neither case protect NCI-H82 and NCI-N592 cells from etoposide-induced apoptosis (Figure 5a–c). To test whether cell adhesion induced by CXCL12 and integrin ligands coplated on plastic is sufficient to enhance etoposide resistance, we used fibronectin and immobilized CXCL12. As previously described by Sethi *et al.* (1999), fibronectin protected the SCLC cells against etoposide-induced apoptosis, but we could not find an additional CXCL12 effect, when cells were cultivated with fibronectin and CXCL12 (data not shown). However, precoating the culture plates with CXCL12 had a significant protective effect on etoposide-induced apoptosis of NCI-N592 cells in serum-free medium (Figure 5c), but this effect could not be seen in full medium with 10% fetal calf serum (FCS) (Figure 5b). Moreover, the integrins were locked in activated state by addition of Manganese ions which led to strong adhesion of the cells to the plates. SCLC cells cultivated in full medium were significantly protected from etoposide-induced apoptosis by the addition of Manganese, whereas there was no protective effect in serum-free medium (Figure 5b and c). As additional controls, SCLC cells were treated with CXCL12 or Manganese without etoposide. In serum-free medium, Manganese reduced the viability of NCI-N592 cells about 30%. This may be one possible explanation for the result that Manganese did not protect the SCLC cells from etoposide-induced apoptosis in serum-free medium.

Stromal cells protect SCLC cells against etoposide-induced apoptosis – antagonization by TN14003

M2-10B4 marrow stromal cells secrete high levels of bioactive CXCL12 (Burger *et al.*, 1999). We previously showed that the adhesion of SCLC cells to stromal cells is dependent on CXCR4/CXCL12 interaction (Burger *et al.*, 2003b). We now investigated the protective effect of marrow stromal cells against etoposide-induced apoptosis of SCLC cells. CXCR4-specific antagonists were used to inhibit the protective effect of stromal cells.

NCI-H82 and NCI-N592 cells were cultivated with or without M2-10B4 cells and treated with 100 μg/ml etoposide or combinations of etoposide and TN14003 (Figure 6a and b). SCLC cells were stained with CD56-PE to distinguish from M2-10B4 cells and cell viability of SCLC cells was determined after 48 h. Growth on M2-10B4 did not improve the viability of NCI-H82 cells, but slightly improved viability of NCI-N592 cells (Figure 6d). Correspondingly, TN14003 treatment (100 μg/ml) did not decrease cell viability of NCI-H82 cells plated on M2, but slightly decreased cell viability of NCI-N592 cells. When cells were treated with etoposide, cell viability after 48 h was between 10 and 30% in comparison to the untreated cells. Coculture of SCLC cells with M2-10B cells protected the cells from etoposide-induced apoptosis and significantly increased the percentage of viable cells. Pretreatment of SCLC cells with TN14003 antagonized the protective effect of the marrow stromal cells, indicating that the protective effect of stromal cells is caused by the CXCR4/CXCL12 interaction.

TN14003 antagonizes the protective effect of the marrow stromal cells supposedly by affecting the CXCL12-induced integrin upregulation and adhesion to stroma. It is known that M2-10B4 cells express integrin ligands laminin, collagen IV and fibronectin (Zipori *et al.*, 1985; Lemoine *et al.*, 1988). VCAM-1 secretion of M2-10B4 cells was from 3 to 6 ng/ml VCAM-1 during the 48 h incubation time in our experimental settings. This high concentration of the $\alpha4\beta1$ ligand VCAM and our previous results on the influence of $\alpha4\beta1$ for the adhesion of SCLC cells to stromal cells (Burger *et al.*, 2003a) suggests a role of $\alpha4$ in the CAM-DR. We tested the contribution of integrin subunits on SCLC by using blocking antibodies to $\alpha4$- and $\alpha5$-integrin subunits. Preincubation of SCLC cells with $\alpha4$ blocking antibody significantly decreased chemoresistance compared to control experiments without blocking antibody (Figure 6c). Pretreatment with $\alpha5$ blocking antibodies had less effect than pretreatment with four blocking antibodies. Altogether, the protective effect of stromal cells is caused by CXCR4 along with integrin activation.

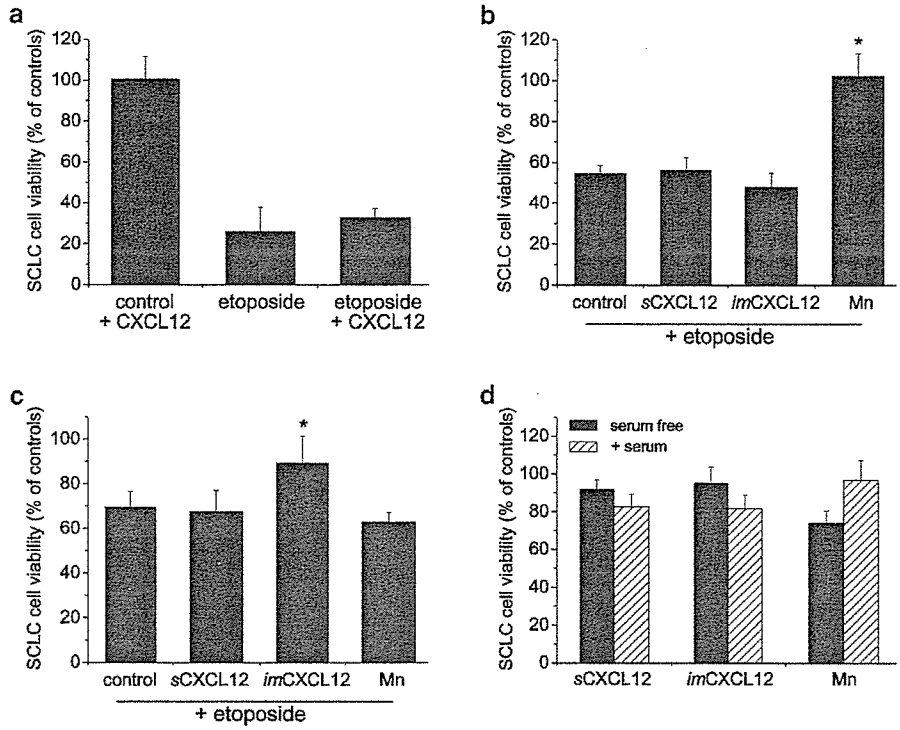

Figure 5 SCLC cells are not protected from etoposid-induced apoptosis by sCXCL12. (a) NCI-H82 cells were treated with 500 ng/ml sCXCL12 and/or 200 μg/ml etoposide for 48 h in full medium. Viability of cells was cytometrically determined with $DIOC_6$ and PI staining of the cells. Values are displayed as percentage of untreated controls. Data represent the mean and standard error of three independent experiments. (**b**) Effects of 500 ng/ml sCXCL12, 800 ng immobilized CXCL12 (imCXCL12) and 1 mM Manganese (Mn) on the viability of NCI-N592 cells after treatment with 100 μg/ml etoposide in full medium for 48 h. Values are displayed as percentage of untreated controls. Data represent the mean and standard error of five independent experiments. (c) Effects of sCXCL12, imCXCL12 and Mn on the viability of NCI-N592 cells after etoposide treatment in serum-free medium. Values are displayed as percentage of untreated controls. Data represent the mean and standard error of at least four independent experiments. (**d**) Effects of sCXCL12, imCXCL12 and Mn on the viability of NCI-N592 in serum-free medium and full medium after 48 h. Values are displayed as percentage of untreated controls. Data represent the mean and standard error of at least four independent experiments

Discussion

Although the majority of advanced stage SCLC patients initially display impressive responses to chemotherapy, SCLC almost invariably relapses, becomes resistant to treatment and therefore remains an incurable disease. Sethi *et al.* (1999) previously demonstrated that adhesion of SCLC cells to accessory cells or ECM within the tumor microenvironment protects SCLC cells from cytotoxic drugs commonly used to treat SCLC patients. This mechanism of primary resistance is, at least partially, mediated via signaling through integrins expressed on SCLC cells and may be responsible for minimal residual disease and relapses. However, integrin activation generally is connected to chemokine receptor activation, a model that initially was developed to explain leukocyte transendothelial migration ('multistep paradigm') (Springer, 1994). It has been shown by several groups that CXCR4 enhances adhesion of hematopoetic cells and tumor cells to vascular endothelium (Peled *et al.*, 1999; Murakami *et al.*, 2002).

Previously we reported that SCLC cells express high levels of functional CXCR4 receptors (Burger *et al.*, 2003b). Here we demonstrate that β1-integrin-dependent resistance mechanisms of SCLC cells are partly mediated by CXCR4 signaling. Our results indicate that CXCL12/CXCR4 are important mediators for the adherence of SCLC cells to ECM proteins like fibronectin, collagen I and VCAM-1. CXCR4-induced adhesion of SCLC cells to marrow stromal cells protected them against etoposide-induced apoptosis. The protective effect of the marrow stromal cells could be antagonized by CXCR4-specific inhibitors and antibodies against α4 integrins.

Looking at signaling components involved in adhesion, we found that CXCL12 treatment induced the phosphorylation of the focal adhesion complex component paxillin. Focal adhesions are structures that mediate adherent contacts with the ECM. In accordance with our results on SCLC cells, paxillin phosphorylation in response to CXCL12 was recently found in breast cancer cells (Fernandis *et al.*, 2004). Paxillin serves as a binding site for a number of important signaling and structuring molecules including vinculin, talin, Crk, Crk-L, p130Cas and Src (Hamasaki *et al.*, 1996; Ganju *et al.*, 1998; Duong and Rodan, 2000; Wade *et al.*, 2002). In contrast to the situation in breast cancer cells (Fernandis *et al.*, 2004), we found constitutive activation of FAK and Crk-L in SCLC cells. Furthermore, our group and others reported that CXCL12 activates PI3 K

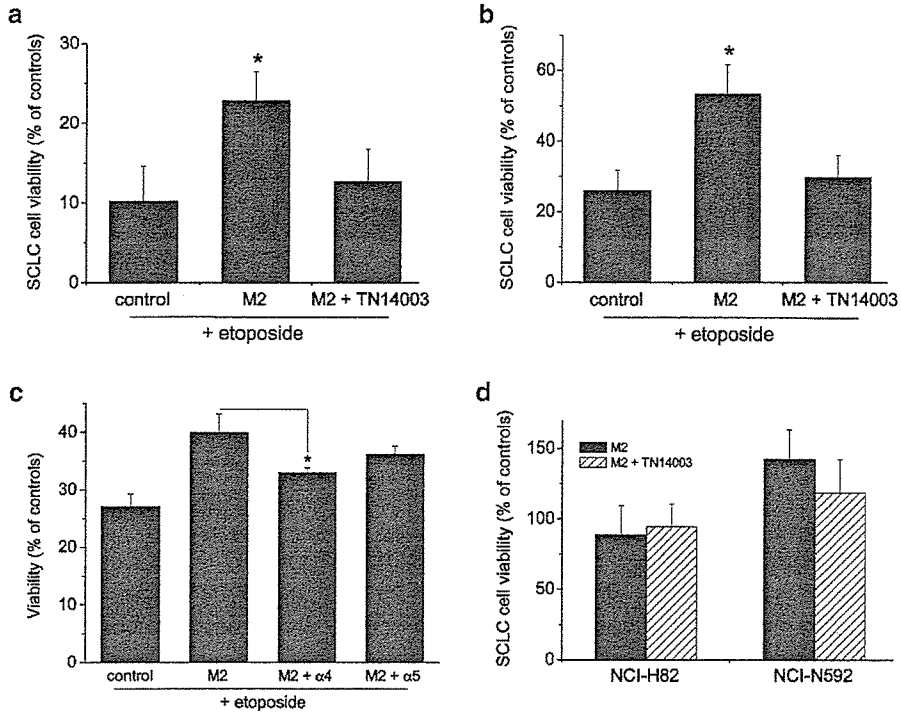

Figure 6 Stromal cells protect SCLC cells against etoposide-induced apoptosis – antagonization by TN14003. NCI-H82 (**a**) and NCI-N592 (**b**) cells were cultivated with or without M2-10B4 cells and treated with 100 μg/ml etoposide or etoposide and TN14003. After 48 h, SCLC cells were stained with CD56-PE to distinguish from M2-10B4 cells and cell viability of SCLC cells was determined. Data represent the mean and s.e.m. of at least five independent experiments. The asterisks indicate significantly higher viabilities compared to the control without M2-10B4 cells ($P \leqslant 0.05$). (**c**) Effect of blocking antibodies against α4- and α5-integrin subunits on the chemoresistance of SCLC cells. NCI-H82 were pretreated with 20 μg/ml anti-α4 or anti-α5 blocking antibodies, cultivated on M2-10B4 cells and treated with 100 μg/ml etoposide. After 48 h, cell viability was determined. Data represent the mean and s.e.m. of four (α4) or five (α5) independent experiments. The asterisk indicates significantly lower viability of α4-antibody-treated cells on M2-10B4 cells compared to untreated controls ($P \leqslant 0.05$). (**d**) Effect of stromal cells and TN14003 on the viability of SCLC cells. NCI-H82 and NCI-N592 cells were cultivated with or without M2-10B4 cells and treated with 100 μg/ml TN14003. After 48 h, cell viability was determined. Values are displayed as percentage of controls (SCLC cells not cultivated on M2-10B4 cells). Data represent the mean and s.e.m. of at least three independent experiments. The asterisks indicate significantly higher viabilities compared to the control without M2-10B4 cells ($P \leqslant 0.05$)

and p44/42 MAP kinase in SCLC cells (Kijima *et al.*, 2002; Burger *et al.*, 2003a). To study whether PI3K was involved in the CXCL12-triggered cell adhesion, we preincubated the cells with the PI3K inhibitor LY294002, which however did not affect the upregulation of adhesion to VCAM-1 by CXCL12. Moreover, the MEK inhibitor PD98059 did not influence CXCL12-induced adhesion, which implies that the MAP kinase pathway does not contribute to integrin activation in SCLC cells. Similar observations have been made in REH pro-B cells, in bone-marrow-derived leukemia and myeloma cell lines (Hidalgo *et al.*, 2001; Sanz-Rodriguez *et al.*, 2001; Glodek *et al.*, 2003).

CXCR4 is a Gαi-coupled receptor, and Pertussis toxin (PT) is an agent that catalyses the ADP ribosylation of specific G protein α subunits of the Gi family, preventing receptor–G protein interactions. However, PT only partially reduced the enhancement of static adhesion of SCLC cells to VCAM-1, fibronectin and collagen coimmobilized with CXCL12. These data indicate that also Gαi-independent signaling must be involved in CXCL12 enhanced adhesion. In accordance with our findings Wright *et al.* (2002) demonstrated in a study on lymphocytes that PT completely blocked chemotaxis, but the $\alpha 4\beta 7$-dependent adhesion of B and T lymphocytes triggered by CXCL12 was only partially inhibited by PT. In the same work Wright *et al.* reported that inhibition of RhoA activation reduced the upregulation of $\alpha 4\beta 7$-dependent adhesion, suggesting that activation of RhoA is an important step in the signaling leading to increased adhesion. This goes in line with our present findings that inhibition of Rho kinase and small Rho GTPases leads to a reduction in CXCL12-triggered adhesion to $\beta 1$ integrins.

The adherence of SCLC cells to ECM proteins fibronectin, collagen I and VCAM-1 is mediated by various integrins. As we demonstrated by using blocking antibodies, activation of $\alpha 2$, but not of $\alpha 1$- or $\alpha 3$-integrin subunits were involved in the CXCL12-induced adhesion to collagen. Both, activation of $\alpha 4$- and $\alpha 5$-integrin subunits contributed to the SCLC adhesion to fibronectin, but blocking the $\alpha 5$ subunit led to a stronger decrease than blocking of the $\alpha 4$ subunit. The CXCL12-induced adhesion to VCAM-1, fibronectin, and collagen

was completely inhibited by pretreatment of the SCLC cells with the CXCR4 antagonist T140, a 14-residue peptide with highly specific CXCR4 antagonistic activities.

Sethi *et al.* (1999) were the first who demonstrated that β1-integrin activation promotes growth and survival of SCLC cells. They found that this β1-integrin-dependent resistance mechanism to chemotherapy was mediated by a protein tyrosine kinase-dependent mechanism. Subsequent, Kraus *et al.* (2002) found that variant SCLC cell lines NCI-H69ad and NCI-N592ad, that have been subcultivated and selected for adherent growth, showed increased chemo- and radio-resistance with constitutive activation of AKT and MAP kinase pathways and upregulation of integrins α2, α3 and β4. In addition, integrin-mediated adhesion of myeloma cells to fibronectin (Hazlehurst *et al.*, 2000) and of glioma cells to vitronectin (Uhm *et al.*, 1999) induced drug resistance. These studies led to the hypothesis that cell–matrix interactions at the tumor–stroma interface are able to confer resistance to apoptosis, a phenomenon referred to as cell adhesion-mediated drug resistance (CAM-DR). Although it has not yet been clearly established whether such a mechanism might account for the acquired resistance found in SCLC, CAM-DR could perhaps explain the local recurrence of SCLC often seen clinically after chemotherapy.

The data of our study suggest that CXCR4 mediates the β1-integrin-dependent adhesion of SCLC cells to ECM proteins. Previously we have shown that stromal cell adhesion of SCLC cells was significantly inhibited by the specific CXCR4 antagonist T140, anti-CXCR4 antibodies, anti-VCAM-1 antibodies, and CS-1 peptide. This demonstrates the involvement of CXCR4 chemokine receptor activation and α4β1-integrin binding in the adhesion of SCLC cells to stroma (Burger *et al.*, 2003b). Marrow stromal cells are a dominant source of CXCL12 *in vivo* and retain their capacity to secrete high amounts of this chemokine *in vitro* (Burger *et al.*, 1999). Here, we demonstrate that the adhesion to marrow stromal cells protected SCLC cells against etoposide-induced apoptosis. This seems to be dependent on CXCR4 and integrin signaling, since pretreatment of SCLC cells with TN14003 and antibodies against α4 integrin could antagonize the protective effect of marrow stromal cells on etoposide-induced apoptosis. Whereas sCXCL12 did not have any effect on the survival of SCLC cells after etoposide treatment, immobilized CXCL12 increased SCLC survival under serum-free culture conditions. This suggests that juxtaposition of the chemokine and integrin ligand is necessary to stimulate integrin-mediated adhesion that leads to the increased chemoresistance. Similar to our observation Grabovsky *et al.* (2000) and Peled *et al.* (1999) demonstrated that for the rapid triggering of VLA-4 adhesions of T lymphocytes or hematopoetic progenitors (HPC) surface-bound CXCL12 was necessary and could not be induced by soluble chemokines.

Locking the integrins in activated state by Manganese had a strong protective effect on etoposide-induced apoptosis in full medium. This suggests, that the integrin activation is sufficient to protect from etoposide-induced apoptosis independent of the factor that induced the activation. For our model on CXCL12-mediated CAM-DR, we suggest that CXCR4 mediates β1-integrin-dependent adhesion to ECM components, which then leads in several other steps, e.g. tyrosine kinase signaling, to resistance. Accordingly, CAM-DR of myeloma cells against mitoxantrone involves cell–cell adhesion of bone marrow stromal cells with myeloma cells as well as soluble factors induced by this cell–cell interaction (Nefedova *et al.*, 2003).

In summary, our results support the concept of CAM-DR described by Sethi *et al.* (1999) and show for the first time the involvement of CXCR4 in this concept. Signals from CXCR4 receptors may induce integrin activation resulting in resistance to chemotherapy-induced apoptosis in SCLC. The CXCR4 antagonist T140 and its derivates blocked the CXCR4-mediated adhesion to ECM components and thereby affected SCLC chemosensitivity. Thus, CXCR4 antagonists like T140 seem to be promising new therapeutic tools for improving the treatment of SCLC.

Materials and methods

Cell culture, chemokines, antibodies

The SCLC cell lines NCI-H82, NCI-H69, NCI-H446, NCI-N592, belonging to the classic subclass of SCLC, and the murine stromal cell line M2-10B4 were obtained from the American Type Culture Collection (ATCC, Manassas, VA, USA). The cells were maintained in RPMI 1640 medium containing 10% FCS and penicillin–streptomycin–glutamine (Gibco-BRL, Grand Island, NY, USA).

Synthetic human CXCL12 was purchased from Upstate Biotechnology (Lake Placid, NY, USA). Etoposide was purchased from Sigma-Aldrich (Munich, Germany). Antibody against phospho-CrkL was purchased from Cell Signalling Technology Inc. (Beverly, MA, USA). Antibodies against CrkL and phosphotyrosine, clone 4G10 were obtained from Upstate Biotechnology. Antibodies against phospho-FAK, FAK and paxillin were purchased from Santa Cruz Biotechnology Inc. (Heidelberg, Germany). The inhibitors T140, a 14 amino-acid residue peptide and its derivates TC14012 and TN14003, that possess higher stability in serum (Tamamura *et al.*, 2001; Fujii *et al.*, 2003), were developed and kindly provided by N Fujii (Kyoto, Japan). PT and PD98059 were purchased from Merck (Darmstadt, Germany). Y27632 was purchased by Tocris Cookson Inc. (Ellisville, MO, USA). Toxin B was friendly provided by K Aktories (Freiburg, Germany).

Immunoprecipitation and Western blotting

SCLC cells were serum starved for 4 h, and lysates from 5×10^6 cells per sample were prepared after stimulation with 100 ng/ml CXCL12 at the indicated time points. Lysis buffer was 20 mM Tris/HCl, pH 8.0, 150 mM KCl, 1 mM EDTA, 0.2 mM Na_3VO_4, 1% Triton X, 0.5 mM PMSF, protein inhibitor cocktail (complete®, Roche Applied Science, Penzberg, Germany). Equal amounts of protein were separated by 10% SDS–polyacrylamide gel electrophoresis (PAGE) and transferred onto PDVF membranes. Western blot analysis was performed using the appropriate antibodies recognizing the

phosphorylated form of the proteins or the total proteins. Immunoreactive bands were visualized using horseradish peroxidase-conjugated secondary antibody and the enhanced chemiluminescence system (Amersham Biosciences, Freiburg, Germany).

For phospho-paxillin detection immunoprecipitations were performed using lysates prepared from SCLC cells. Phosphotyrosine antibodies (3.5 μg) were added; and the samples were incubated overnight at 4°C. Immunoprecipitates were collected with 30 μl Protein G Sepharose beads (Zymed, San Francisco, CA, USA) for 2 h at 4°C. They were washed three times with lysis buffer, fractionated by SDS–PAGE and immunoblotted with paxillin antibody.

SCLC cell adhesion to immobilized VCAM-1, fibronectin and collagen

In all, 96-well plates (Nalge Nunc International, Rochester, NY, USA) were coated with recombinant human VCAM-1 (R&D Systems, Minneapolis, MN, USA, 1.3 μg/ml) or fibronectin (BD Biosciences, Heidelberg, Germany, 10 μg/ml) or Collagen I (Sigma-Aldrich, Munich, Germany, 5 μg/ml) prepared in bicarbonate buffer (pH 9.6) and incubated overnight at 4°C. Wells were then washed three times with bicarbonate buffer and coated with recombinant human CXCL12 prepared at 8.0 μg/ml in bicarbonate buffer for 30 min at room temperature or with the buffer alone. Wells were subsequently washed and blocked with 1% tissue culture BSA (Sigma) in PBS for 1 h at 37°C, followed by washing with Hank's Balanced Salt Solution (HBSS) supplemented with 10 mM HEPES, pH 8.0. Cells were preincubated with different inhibitors, washed in PBS and resuspended at 10^5 per 50 μl of adhesion medium (HBSS buffered with HEPES and supplemented with 0.5% BSA). Cells were added in quatriplicate to the wells and allowed to settle for 30 min at 37°C, followed by four washes with adhesion medium to remove nonadhered cells. The number of adhered cells was determined using CyQUANT Cell Proliferation Kit (Molecular Probes, Eugene, OR, USA) and fluorescence of the samples was measured by a Microtiter Plate Fluorometer.

Measurement of cell viability and expression of integrin subunits

For all experiments, viability of SCLC cells was routinely determined by trypan blue exclusion. In chemosensitivity experiments, determination of SCLC cell viability was based on the analysis of mitochondrial transmembrane potential by 3,3′ dihexyloxacarbocyanine iodine ($DIOC_6$) and cell membrane permeability to propidium iodide (PI). In all, 48-well plates were precoated with 100 μl 8 μg/ml CXCL12 or BSA (controls). Cells were resuspended at 10^5 per 500 μl of serum-free RPMI or full medium. In all, 500 ng/ml CXCL12 and 1 mM $MnCl_2$ was added where indicated. After 48 h SCLC cells were collected and viability was determined in RPMI 1640 containing 0.5% BSA, 10 nM $DIOC_6$ (Molecular Probes) and 2 μg/ml PI (Molecular Probes) in RPMI 1640, 0.5% BSA. Cells were then incubated at 37°C for 20 min and analysed within 30 min by flow cytometry on a FACSCalibur (Becton Dickinson, Mountain View, CA, USA). Flow cytometry data were analysed using the FlowJo 3.3 software (Tree Star Inc., San Carlos, CA, USA).

Expression of integrins was determined using monoclonal anti-CD49a, anti-CD49b, anti-Cd49c, anti-CD49d, anti-CD49e and anti-CD29 antibodies and the appropriate isotype controls from Chemicon International Inc. (Temecula, CA, USA). SCLC cells were adjusted to a concentration of 10^6 cells/ml in RPMI 1640, 0.5% BSA. A total of 10^5 cells was stained with saturating antibody concentrations for 30 min at 4°C and afterwards washed two times. In cases of indirect antibody labeling, cells were incubated with appropriate secondary antibody and again washed two times. Integrin expression was analysed on the FACSCalibur.

SCLC-stromal cell adhesion assay

The murine stromal cell line M2-10B4 that secretes high amounts of CXCL12 (Burger *et al*., 1999) was seeded the day before the assay onto 24-well plates at a concentration of 0.5×10^5 cells per well in RPMI-1640 supplemented with 10% FCS. In some cases, SCLC cells were preincubated with 100 μg/ml TN14003 or 20 μg/ml blocking antibodies against α4-, α5- or β1-integrin subunits for 30 min at 37°C, and seeded on the stromal cell layer at a concentration of 2×10^5 cells per well. Controls were seeded onto 24-well plates without stromal cells. After 4 h at 37°C in 5% CO_2, cells were treated with 100 μg/ml etoposide and incubated for another 48 h at 37°C. In order to distinguish SCLC cells from stromal cells during the flow cytometry-based analysis of SCLC cell adhesion to stromal cells, SCLC cells were labeled with CD56-PE for 30 min at 4°C and afterwards incubated with 100 nM $DIOC_6$ in RPMI 1640 medium with 0.5% BSA. Viability of SCLC cells was analysed by flow cytometry.

Statistical analysis

For statistical analysis, the paired Student's *t*-test for comparison of two groups was used. Analyses were performed with the statistic tool of Origin 7G, OriginLab Corporation (Northampton, MA, USA). Values were considered significant when $P<0.05$.

Acknowledgements
The authors are grateful to Myriam Krome and Barbara Rogalsky for excellent technical assistance. Supported by the Deutsche Forschungsgemeinschaft (DFG) grant no. BU/1159/3-2 (to MB), and Deutsche Krebshilfe grant no. 10-1688-Bu (to JAB).

References

Burger JA, Burger M and Kipps TJ. (1999). *Blood*, **94**, 3658–3667.
Burger JA, Spoo A, Dwenger A, Burger M and Behringer D. (2003a). *Br. J. Haematol.*, **122**, 579–589.
Burger M, Glodek A, Hartmann T, Schmitt-Graff A, Silberstein LE, Fujii N, Kipps TJ and Burger JA. (2003b). *Oncogene*, **22**, 8093–8101.
Campbell JJ, Hedrick J, Zlotnik A, Siani MA, Thompson DA and Butcher EC. (1998). *Science*, **279**, 381–384.
Constantin G, Majeed M, Giagulli C, Piccio L, Kim JY, Butcher EC and Laudanna C. (2000). *Immunity*, **13**, 759–769.
Duong LT and Rodan GA. (2000). *Cell Motil. Cytoskeleton*, **47**, 174–188.
Fernandis AZ, Prasad A, Band H, Klosel R and Ganju RK. (2004). *Oncogene*, **23**, 157–167.
Fujii N, Nakashima H and Tamamura H. (2003). *Expert Opin. Invest. Drugs*, **12**, 185–195.

Ganju RK, Brubaker SA, Meyer J, Dutt P, Yang Y, Qin S, Newman W and Groopman JE. (1998). *J. Biol. Chem.*, **273,** 23169–23175.

Geminder H, Sagi-Assif O, Goldberg L, Meshel T, Rechavi G, Witz IP and Ben-Baruch A. (2001). *J. Immunol.*, **167,** 4747–4757.

Glodek AM, Honczarenko M, Le Y, Campbell JJ and Silberstein LE. (2003). *J. Exp. Med.*, **197,** 461–473.

Grabovsky V, Feigelson S, Chen C, Bleijs DA, Peled A, Cinamon G, Baleux F, Arenzana-Seisdedos F, Lapidot T, van Kooyk Y, Lobb RR and Alon R. (2000). *J. Exp. Med.*, **192,** 495–506.

Hamasaki K, Mimura T, Morino N, Furuya H, Nakamoto T, Aizawa S, Morimoto C, Yazaki Y, Hirai H and Nojima Y. (1996). *Biochem. Biophys. Res. Commun.*, **222,** 338–343.

Hazlehurst LA, Damiano JS, Buyuksal I, Pledger WJ and Dalton WS. (2000). *Oncogene*, **19,** 4319–4327.

Hidalgo A, Sanz-Rodriguez F, Rodriguez-Fernandez JL, Albella B, Blaya C, Wright N, Cabanas C, Prosper F, Gutierrez-Ramos JC and Teixido J. (2001). *Exp. Hematol.*, **29,** 345–355.

Hoffman PC, Mauer AM and Vokes EE. (2000). *Lancet*, **355,** 479–485.

Ihde DC. (1992). *N. Engl. J. Med.*, **327,** 1434–1441.

Kijima T, Maulik G, Ma PC, Tibaldi EV, Turner RE, Rollins B, Sattler M, Johnson BE and Salgia R. (2002). *Cancer Res.*, **62,** 6304–6311.

Kraus AC, Ferber I, Bachmann SO, Specht H, Wimmel A, Gross MW, Schlegel J, Suske G and Schuermann M. (2002). *Oncogene*, **21,** 8683–8695.

Lassen U, Osterlind K, Hansen M, Dombernowsky P, Bergman B and Hansen HH. (1995). *J. Clin. Oncol.*, **13,** 1215–1220.

Lemoine FM, Humphries RK, Abraham SD, Krystal G and Eaves CJ. (1988). *Exp. Hematol.*, **16,** 718–726.

Muller A, Homey B, Soto H, Ge N, Catron D, Buchanan ME, McClanahan T, Murphy E, Yuan W, Wagner SN, Barrera JL, Mohar A, Verastegui E and Zlotnik A. (2001). *Nature*, **410,** 50–56.

Murakami T, Maki W, Cardones AR, Fang H, Tun Kyi A, Nestle FO and Hwang ST. (2002). *Cancer Res.*, **62,** 7328–7334.

Nefedova Y, Landowski TH and Dalton WS. (2003). *Leukemia*, **17,** 1175–1182.

Peled A, Grabovsky V, Habler L, Sandbank J, Arenzana-Seisdedos F, Petit I, Ben-Hur H, Lapidot T and Alon R. (1999). *J. Clin. Invest.*, **104,** 1199–1211.

Phillips RJ, Burdick MD, Lutz M, Belperio JA, Keane MP and Strieter RM. (2003). *Am. J. Respir Crit. Care Med.*, **167,** 1676–1686.

Robledo MM, Bartolome RA, Longo N, Rodriguez-Frade JM, Mellado M, Longo I, van Muijen GN, Sanchez-Mateos P and Teixido J. (2001). *J. Biol. Chem.*, **276,** 45098–45105.

Salgia R, Li JL, Ewaniuk DS, Wang YB, Sattler M, Chen WC, Richards W, Pisick E, Shapiro GI, Rollins BJ, Chen LB, Griffin JD and Sugarbaker DJ. (1999). *Oncogene*, **18,** 67–77.

Sanz-Rodriguez F, Hidalgo A and Teixido J. (2001). *Blood*, **97,** 346–351.

Schaller MD. (2001). *Biochim. Biophys. Acta*, **1540,** 1–21.

Sethi T, Rintoul RC, Moore SM, MacKinnon AC, Salter D, Choo C, Chilvers ER, Dransfield I, Donnelly SC, Strieter R and Haslett C. (1999). *Nat. Med.*, **5,** 662–668.

Springer TA. (1994). *Cell*, **76,** 301–314.

Taichman RS, Cooper C, Keller ET, Pienta KJ, Taichman NS and McCauley LK. (2002). *Cancer Res.*, **62,** 1832–1837.

Tamamura H, Omagari A, Hiramatsu K, Gotoh K, Kanamoto T, Xu Y, Kodama E, Matsuoka M, Hattori T, Yamamoto N, Nakashima H, Otaka A and Fujii N. (2001). *Bioorg. Med. Chem. Lett.*, **11,** 1897–1902.

Uhm JH, Dooley NP, Kyritsis AP, Rao JS and Gladson CL. (1999). *Clin. Cancer Res.*, **5,** 1587–1594.

Vicente-Manzanares M, Montoya MC, Mellado M, Frade JM, del Pozo MA, Nieto M, de Landazuri MO, Martinez AC and Sanchez-Madrid F. (1998). *Eur. J. Immunol.*, **28,** 2197–2207.

Wade R, Bohl J and Vande Pol S. (2002). *Oncogene*, **21,** 96–107.

Wright N, Hidalgo A, Rodriguez-Frade JM, Soriano SF, Mellado M, Parmo-Cabanas M, Briskin MJ and Teixido J. (2002). *J. Immunol.*, **168,** 5268–5277.

Zipori D, Toledo J and von der Mark K. (1985). *Blood*, **66,** 447–455.

Stereoselective Synthesis of [L-Arg-L/D-3-(2-naphthyl)alanine]-Type (*E*)-Alkene Dipeptide Isosteres and Its Application to the Synthesis and Biological Evaluation of Pseudopeptide Analogues of the CXCR4 Antagonist FC131

Hirokazu Tamamura,*,† Kenichi Hiramatsu,† Satoshi Ueda,† Zixuan Wang,‡ Shuichi Kusano,§ Shigemi Terakubo,§ John O. Trent,‖ Stephen C. Peiper,‡ Naoki Yamamoto,⊥ Hideki Nakashima,§ Akira Otaka,† and Nobutaka Fujii*,†

Graduate School of Pharmaceutical Sciences, Kyoto University, Sakyo-ku, Kyoto 606-8501, Japan, Medical College of Georgia, Augusta, Georgia 30912, St. Marianna University, School of Medicine, Miyamae-ku, Kawasaki 216-8511, Japan, James Graham Brown Cancer Center, University of Louisville, Louisville, Kentucky 40202, and Tokyo Medical and Dental University, School of Medicine, Bunkyo-ku, Tokyo 113-8519, Japan

Received July 18, 2004

L,L-Type and L,D-type (*E*)-alkene dipeptide isosteres (EADIs) that have unnatural side chains at the α-position were synthesized by the combination of stereoselective aziridinyl ring-opening reactions and organozinc−copper-mediated *anti*-S_N2' reactions toward a single substrate of γ,δ-*cis*-γ,δ-epimino (*E*)-α,β-enoate. The utility of this methodology was demonstrated by the stereoselective synthesis of a set of diastereomeric EADIs of L-Arg-L/D-3-(2-naphthyl)alanine (Nal) that is contained in a small CXCR4 antagonist FC131 [*cyclo*(-D-Tyr-Arg-Arg-Nal-Gly-)]. Furthermore, a (Nal-Gly)-type EADI was synthesized by samarium diiodide (SmI_2)-induced reduction of a γ-acetoxy-α,β-enoate. Several FC131 analogues, in which these EADIs were inserted for reduction of their peptide character, were synthesized with analogues containing reduced amide-type dipeptide isosteres to investigate the importance of these amide bonds for anti-HIV and CXCR4-antagonistic activity.

Introduction

The practical utility of (*E*)-alkene dipeptide isosteres (EADIs) has been intensively investigated in structure−activity relationship (SAR) studies of biologically active peptides toward development of peptide-lead drugs.[1−7] Backbone replacements of amide bonds in peptides by EADIs provide information on the contributions of the corresponding amide bonds on biological activity. We previously established a completely stereocontrolled synthetic process for L,L-type and L,D-type EADIs starting from L-amino acid.[8,9] As shown in Scheme 1, treatment of *N*-aryl-γ,δ-*cis*-γ,δ-epimino (*E*)-α,β-enoates (*cis*-(*E*)-enoates) **1** with methanesulfonic acid (MSA) gives γ-mesyloxy-α,β-enoates **2**, which can be converted into L,D-type EADIs **3** by organocopper-mediated α-alkylation via *anti*-S_N2' reactions, whereas organocopper treatment of *cis*-(*E*)-enoates **1** affords L,L-type EADIs **4**. However, this synthetic procedure has not yet been optimized, because it involves a potential limitation on the introduction of functional groups into the side chain (R^3) at the α-position. In a standard procedure, organocopper reagents, which were prepared by CuCN and RLi or RMgX (X = Cl or Br), are used for α-alkylation.[2,4] In the α-alkylation of the synthesis of (Xaa-L/D-Glu)-type EADIs,[10] organozinc−copper reagents are used, which are prepared from $IZnCH_2CH_2CO_2R$ and

Scheme 1[a]

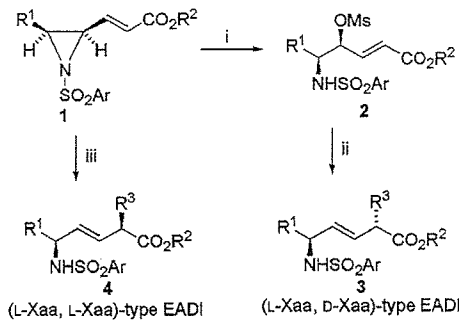

[a] R^1, R^2, R^3 = alkyl; Ar = 2,4,6-trimethylphenylsulfonyl (Mts) or Ts. Reagents: (i) MsOH; (ii) $R^3Cu(CN)MgX\cdot BF_3$ (X = Cl or Br) or $R^3Cu(CN)Li\cdot BF_3$; (iii) $R^3Cu(CN)MgX\cdot 2LiX$ (X = Cl or Br) or $R^3Cu(CN)Li\cdot 2LiX$.

CuCN.[11−15] In this study, to demonstrate the general utility of organozinc−copper reagents, a set of EADIs of L-Arg-L/D-3-(2-naphthyl)alanine (Nal) were synthesized as model compounds via the γ,δ-*cis*-γ,δ-epimino (*E*)-α,β-enoate by the combination of MSA-mediated aziridinyl ring-opening reactions and α-alkylation with organozinc−copper reagents, which were prepared from 2-naphthylmethylZnBr and CuCN. The dipeptide sequence, Arg-Nal, is part of the low molecular weight CXCR4 antagonist, FC131, which was recently developed by us (Figure 1).[16]

CXCR4 is a chemokine receptor, which is involved in cell progression and metastasis of several types of cancer,[17−19] HIV entry,[20] and rheumatoid arthritis.[21,22] Thus, several inhibitors directed against CXCR4 have been developed.[23−27] We previously found a highly potent CXCR4 antagonist, T140, which is a 14-mer

* Corresponding authors. Tel: +81 75 753 4551, Fax: +81 75 753 4570, E-mail: tamamura@pharm.kyoto-u.ac.jp; nfujii@pharm.kyoto-u.ac.jp.
† Kyoto University.
‡ Medical College of Georgia.
§ St. Marianna University.
‖ University of Louisville.
⊥ Tokyo Medical and Dental University.

10.1021/jm049429h CCC: $30.25
Published on Web 12/21/2004

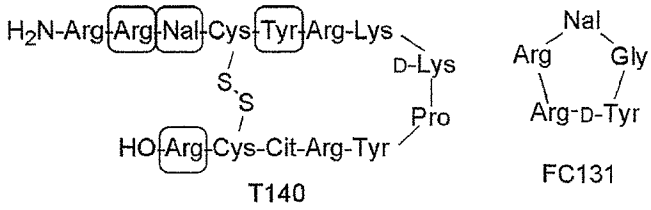

Figure 1. Structures of T140 and its downsized peptide FC131. Circled residues are the indispensable residues of T140 for the expression of strong CXCR4-antagonistic activity. Nal = L-3-(2-naphthyl)alanine, Cit = L-citrulline.

peptide with a disulfide bridge, and we identified four critical residues: Arg^2, Nal^3, Tyr^5, and Arg^{14} (Figure 1).[28-30] Molecular-size reduction of T140 based on the structural requirement led to the discovery of FC131, which has a cyclic pentapeptide template,[31-37] with CXCR4-antagonistic and anti-HIV activity comparable to those of T140.[16] We wish to investigate contributions of each amide bond in FC131 to the biological activity in order to develop pseudopeptides, in which the peptide character is reduced to obtain more druglike structures. For this purpose, EADIs and reduced amide-type dipeptide isosteres (RADIs) of Arg-Nal and Nal-Gly are required, because the amide bonds between Arg^2 and Nal^3 and between Nal^3 and Cys^4 were found to be cleaved by treatment of T140 analogues with rat liver homogenates.[38,39] Thus, (L-Arg-L/D-Nal)-type EADIs were synthesized in the study described here, and a (Nal-Gly)-type EADI was also synthesized by another method using the samarium diiodide (SmI_2)-induced reduction of a γ-acetoxy-α,β-enoate.[40,41] RADIs of Arg-Nal and Nal-Gly were prepared by a standard method of reductive amination. Then, several FC131 analogues, in which the above isosteres were introduced, were synthesized to identify the biological importance of these amide bonds.

Results and Discussion

Synthesis of (L-Arg-L/D-Nal)-Type EADIs. (L-Arg-L/D-Nal)-type EADIs were synthesized via the same key intermediate *N*-2-nitrobenzenesulfonyl (Ns)-γ,δ-*cis*-γ,δ-epimino (*E*)-α,β-enoate, **9**, as synthetic model compounds for the investigation of the feasibility of α-alkylation using organozinc−copper reagents as well as precursor dipeptide isosteres used for the synthesis of partial nonpeptide analogues of FC131 (Scheme 2). Boc-Arg(Mts)-OMe (Mts = 2,4,6-trimethylbenzenesulfonyl) **5** was treated successively with diisobutylaluminum hydride (DIBAL-H) and vinylmagnesium chloride (CH_2=CHMgCl) to give exclusively the *threo*-amino alcohol **6** (a separable mixture of allyl alcohol **6**/*erythro*-isomer of **6** = 12:1). N^{α}-Ns protection[42,43] after the cleavage of the N^{α}-Boc group of **6** with HCl/dioxane followed by successive treatments consisting of the Mitsunobu reaction,[44] ozonolysis, and the modified Horner−Wadsworth−Emmons olefination[45] afforded *cis*-(*E*)-enoate **9**. *Anti*-S_N2' reaction of **9** with an organozinc−copper reagent,[11-15] 2-naphthylmethylCu(CN)-ZnBr·2LiCl, afforded an L,L-type EADI **10**, in which a (2*R*)-2-naphthylmethyl side chain was incorporated at the α-position, stereoselectively in 83% yield (diastereoselection > 99:1 from NMR analysis). N^{α}-Fmoc substitution for the N^{α}-Ns group of **10** followed by selective deprotection of the benzyl ester using thioanisole/TFA afforded a desired EADI, Fmoc-L-Arg(Mts)-ψ[(*E*)-CH=CH]-L-Nal-OH, **12**. Alternatively, exposure of **9** to MSA/$CHCl_3$ afforded exclusively δ-aminated γ-mesyloxy-α,β-enoate **13** by regio- and stereoselective S_N2 ring-opening reaction at the γ-carbon of **9**. Mesylate **13** was successively treated by an organozinc−copper reagent, 2-naphthylmethylCu(CN)ZnBr·BF_3, to afford an L,D-type EADI **14**, in which a (2*S*)-2-naphthylmethyl side chain was incorporated at the α-position, stereoselectively via an *anti*-S_N2'mechanism in 67% yield (diastereoselection > 99:1 from NMR analysis). **14** was similarly converted into another desired EADI, Fmoc-L-Arg(Mts)-ψ[(*E*)-CH=CH]-D-Nal-OH, **16**. As such, α-alkylation of both a *cis*-(*E*)-enoate and its ring-opened product using organozinc−copper reagents was successfully performed in the synthesis of (L-Arg-L/D-Nal)-type EADIs. An *N*-Ns group could be used in this synthetic scheme as an orthogonal *N*-protecting (activating) group instead of an *N*-Mts or *N*-Ts group. Relative configurations of the allyl alcohols (**6** and its erythro isomer) were determined by comparative nuclear Overhauser effect (NOE) measurements of these oxazolidinone derivatives **17** and **18** (Scheme 2).[2] The (*E*)-geometry of the double bond in the synthesized EADIs was assigned based on the coupling constant of the two olefinic protons on ^1H NMR analysis.

Synthesis of (L-Nal-Gly)-Type EADI. An (L-Nal-Gly)-type EADI was synthesized as shown in Scheme 3. Boc-L-Nal-OMe **19** was treated sequentially with DIBAL-H and CH_2=CHMgCl to give a diastereomixture of allyl alcohol **20**. Acetylation of **20** followed by ozonolysis and the modified Horner−Wadsworth−Emmons olefination afforded a γ-acetoxy-α,β-unsaturated ester **22**. Acetate **22** was reduced with SmI_2−^{t}BuOH to yield an (L-Nal-Gly)-type EADI **23** in 95% yield,[40,41] followed by deprotection of the N^{α}-Boc group and *tert*-butyl ester with TFA and reprotection with an N^{α}-Fmoc group to afford the desired EADI, Fmoc-L-Nal-ψ[(*E*)-CH=CH]-Gly-OH, **24**.

Synthesis of RADIs of Arg-Nal and Nal-Gly. (L-Arg-L-Nal)- and (L-Nal-Gly)-type RADIs were prepared for comparative studies. As shown in Scheme 4, Arg- and Nal-derived Weinreb amides **25** and **29** were treated with DIBAL-H to afford the corresponding aldehyde derivatives. Subsequently, reductive amination of the aldehydes was performed by treatments with carboxy-protected amino acids in the presence of acetic acid and sodium triacetoxy borohydride [$NaBH(OAc)_3$] to afford secondary amines **26** and **30**, respectively.[46] Protection of the *sec*-amino groups with Cbz groups followed by deprotection of the N^{α}-Boc group and *tert*-butyl ester with TFA and reprotection with an N^{α}-Fmoc group afforded the desired RADIs, Fmoc-L-Arg(Mts)-ψ-[CH_2−N(Cbz)]-L-Nal-OH, **28**, and Fmoc-L-Nal-ψ[CH_2−N(Cbz)]-Gly-OH, **32**, respectively.

Synthesis of Cyclic Pseudopeptides. The protected peptide chains were constructed on a hydrazino resin **34** by Fmoc-based solid-phase synthesis using ^{t}Bu and 2,2,4,6,7-pentamethyldihydrobenzofuran-5-sulfonyl (Pbf) groups for side-chain protection of D-Tyr and Arg, respectively (Scheme 5). N^{α}-Fmoc-protected dipeptide isosteres, EADIs **12**, **16**, and **24** and RADIs **28** and **32**, were similarly condensed. In the synthesis of cyclic pseudopeptides, two steps of deprotection/cleavage were adopted to prevent guanidino groups of Arg from

Scheme 2[a]

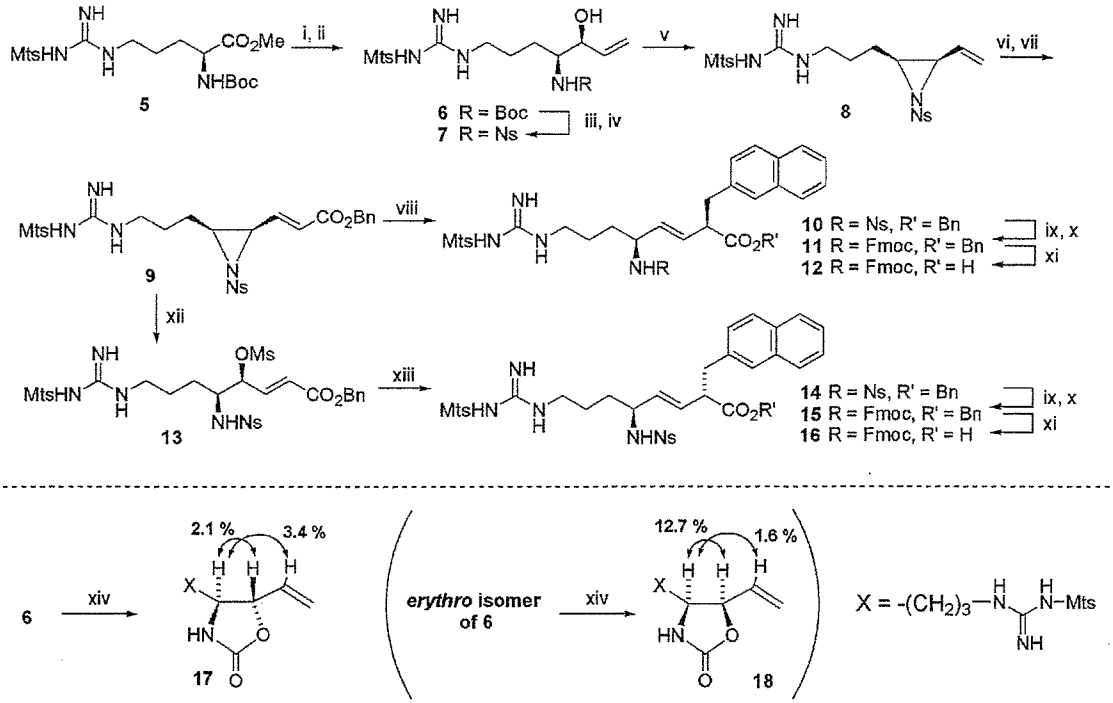

[a] Reagents: (i) DIBAL-H; (ii) CH_2=CHMgCl; (iii) HCl, anisole; (iv) Ns-Cl, pyridine; (v) Ph_3P, DEAD; (vi) O_3, then Me_2S; (vii) $(EtO)_2P(O)CH_2CO_2Bn$, LiCl, DIPEA; (viii) 2-naphthylmethylCu(CN)ZnBr·2LiCl; (ix) PhSH, K_2CO_3; (x) Fmoc-OSu, Et_3N; (xi) thioanisole, TFA; (xii) MsOH; (xiii) 2-naphthylmethylCu(CN)ZnBr·BF_3; (xiv) NaH.

Scheme 3[a]

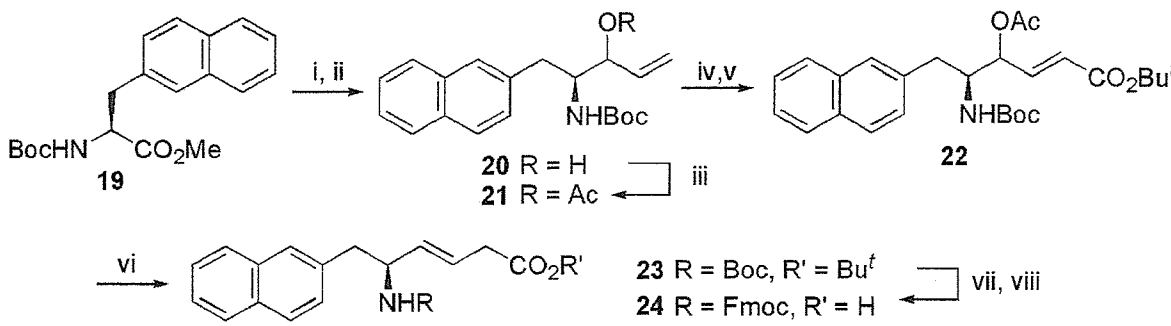

[a] Reagents: (i) DIBAL-H; (ii) CH_2=CHMgCl; (iii) Ac_2O, DMAP, pyridine; (iv) O_3, then Me_2S; (v) $(EtO)_2P(O)CH_2CO_2{}^tBu$, LiCl, DIPEA; (vi) SmI_2, ^tBuOH; (vii) anisole, TFA; (viii) Fmoc-OSu, Et_3N.

Scheme 4[a]

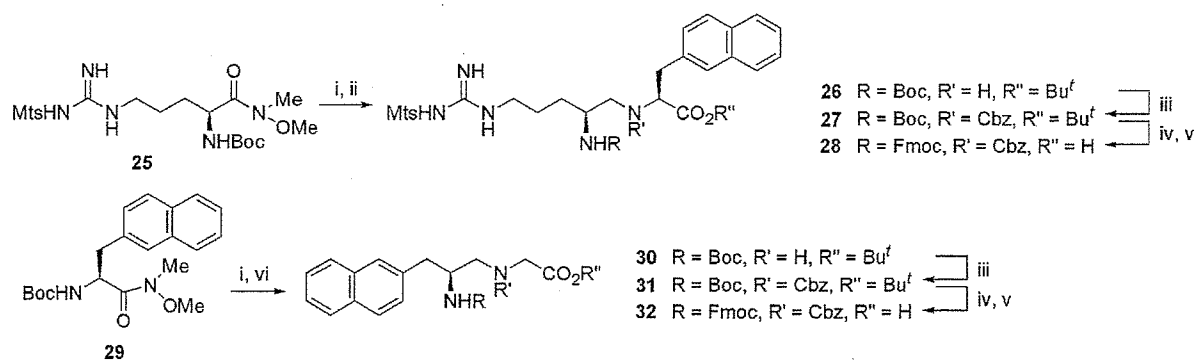

[a] Reagents: (i) DIBAL-H; (ii) H-Nal-O^{t}Bu, AcOH, $NaBH(OAc)_3$; (iii) Cbz-Cl, Et_3N; (iv) anisole, TFA; (v) Fmoc-OSu, Et_3N; (vi) H-Gly-O^{t}Bu, AcOH, $NaBH(OAc)_3$.

participating in cyclizing reaction as follows. After construction of peptide chains, pseudopeptide hydrazides **36** were obtained by cleavage from the resin **35** using 10% TFA/$CHCl_3$ without cleavage of Pbf, Mts, and Cbz groups (first deprotection). Cyclization of linear pseudopeptides by the azide procedure[47] in highly

Scheme 5[a]

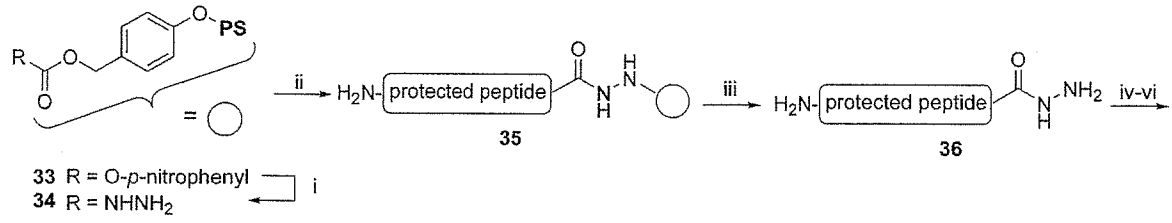

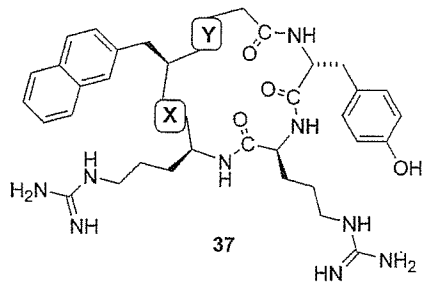

Compd.	Sequence (*cyclo*)	X	Y
FC131	(-D-Tyr-Arg-Arg-Nal-Gly-)	-CO-NH-	-CO-NH-
37a	(-D-Tyr-Arg-Arg-Nal-Gly-)	-CH=CH-	-CO-NH-
37b	(-D-Tyr-Arg-Arg-Nal-Gly-)	$-CH_2$-NH-	-CO-NH-
37c	(-D-Tyr-Arg-Arg-Nal-Gly-)	-CO-NH-	-CH=CH-
37d	(-D-Tyr-Arg-Arg-Nal-Gly-)	-CO-NH-	$-CH_2$-NH-
37e	(-D-Tyr-Arg-Arg-D-Nal-Gly-)	-CO-NH-	-CO-NH-
37f	(-D-Tyr-Arg-Arg-D-Nal-Gly-)	-CH=CH-	-CO-NH-

[a] Reagents: (i) $NH_2NH_2 \cdot H_2O$; (ii) Fmoc-based SPPS; (iii) TFA; (iv) HCl, isoamyl nitrite; (v) DIPEA; (vi) 1 M TMSBr–thioanisole/TFA, *m*-cresol, 1,2-ethanedithiol.

Table 1. Activity and Cytotoxicity of the Synthetic Compounds

compound (no.)	CC_{50}[a] (μM)	EC_{50}[b] (μM)	IC_{50}[c] (μM)
FC131	> 100	0.073	0.0045 ± 0.0018
37a	> 100	2.4	31–100[d]
37b	> 100	> 100	> 100
37c	> 100	2.4	0.18 ± 0.10
37d	> 100	0.98	0.032 ± 0.011
37e	> 100	1.9	0.19 ± 0.071
37f	> 100	9.1	21
T140	> 10	0.035	0.0039 ± 0.0004
AZT	57	0.018	

[a] CC_{50} values are based on the reduction of the viability of mock-infected MT-4 cells. Because the cytotoxicity of T140 was previously evaluated as CC_{50} > 40 μM, further estimation at high concentrations was omitted in this study. [b] EC_{50} values are based on the inhibition of HIV-induced cytopathogenicity in MT-4 cells. [c] IC_{50} values are based on the inhibition of [^{125}I]-SDF-1-binding to CXCR4 transfectants of CHO cells. All data are the mean values for at least three independent experiments. [d] **37a** showed significant antagonistic activity in 100 μM but hardly showed activity in 31 μM.

diluted dimethylformamide (DMF) solution followed by deprotection of Pbf, Mts, and Cbz groups with 1 M TMSBr–thioanisole/TFA (second deprotection) gave the desired cyclic pseudopeptides **37**.

Biological and Conformational Evaluation of Synthetic Cyclic Pseudopeptides. Anti-HIV activity based on the inhibition of HIV-1-induced cytopathogenicity in MT-4 cells was evaluated using the 3-(4,5-dimethylthiazol-2-yl)-2,5-diphenyltetrazolium bromide (MTT) method.[48] CXCR4-antagonistic activity was evaluated by the inhibition of [^{125}I]-SDF-1-binding to CXCR4 transfectants of CHO cells.[49] **37a**, an (L-Arg-L-Nal)-type EADI containing FC131 analogue, showed moderate anti-HIV activity (EC_{50} = 2.4 μM) and CXCR4-antagonistic activity (100 μM > IC_{50} > 31 μM). Introduction of an EADI into the Arg-Nal sequence caused a remarkable decrease in anti-HIV activity (33-fold lower activity). NMR and simulated annealing molecular dynamics (SA-MD) analysis of **37a** showed a pseudopeptide backbone structure with a nearly symmetrical pentagonal shape similar to that of FC131,[16] excluding the difference between the orientation of two protons in the (*E*)-alkene unit of **37a** and that of the carbonyl oxygen/amino proton in the Arg-Nal amide bond of FC131 (Figure 2a).[50] Substitution for the amide bond with the EADI caused an inversion of the olefinic plane (180° rotation of pseudo ψ and ϕ bonds), possibly due to dissolution of the 1,3-pseudo-allylic strain between the carbonyl group of Arg and the side chain of Nal. Introduction of an EADI into the Arg-D-Nal sequence of **37e** (an FC131 epimer, EC_{50} = 1.9 μM, IC_{50} = 190 nM) also caused a significant but moderate decrease in anti-HIV activity (the activity of **37f** is 5-fold lower than that of **37e**). The amide bonds of the Arg-L/D-Nal sequences were necessary for high potency. These results suggested that either a deletion of the hydrogen bond interaction with CXCR4 by the insertion of an EADI or an increase in hydrophobicity might be unsuitable. **37b**, an (L-Arg-L-Nal)-type RADI-containing FC131 analogue, did not show anti-HIV or CXCR4-antagonistic activity up to the concentration of 100 μM, suggesting that the planar nature of the amide bond is critical to maintain the pentagonal global conformation for high anti-HIV activity and that the replacement of the amide bond with RADI causes a conformational change of FC131. **37c**, an (L-Nal-Gly)-type EADI-containing FC131 analogue, showed almost the same anti-HIV activity (EC_{50} = 2.4 μM) as **37a** containing an (L-Arg-L-Nal)-type EADI. NMR and SA-MD analysis of **37c** showed a similar backbone structure with FC131 (Figure 2b).[50] The Nal-Gly amide bond was replaced by the EADI without an inversion of the olefinic plane. **37d**, an (L-Nal-Gly)-type RADI-containing FC131 analogue, exhibited relatively higher anti-HIV and CXCR4-antagonistic activities (EC_{50} = 0.98 μM, IC_{50} = 32 nM) than **37c** (IC_{50} = 180 nM), although these activities were weaker than those of FC131. These results also indicated an importance of the amide bond of the Nal-Gly sequence, as in the case of the Arg-Nal amide bond.

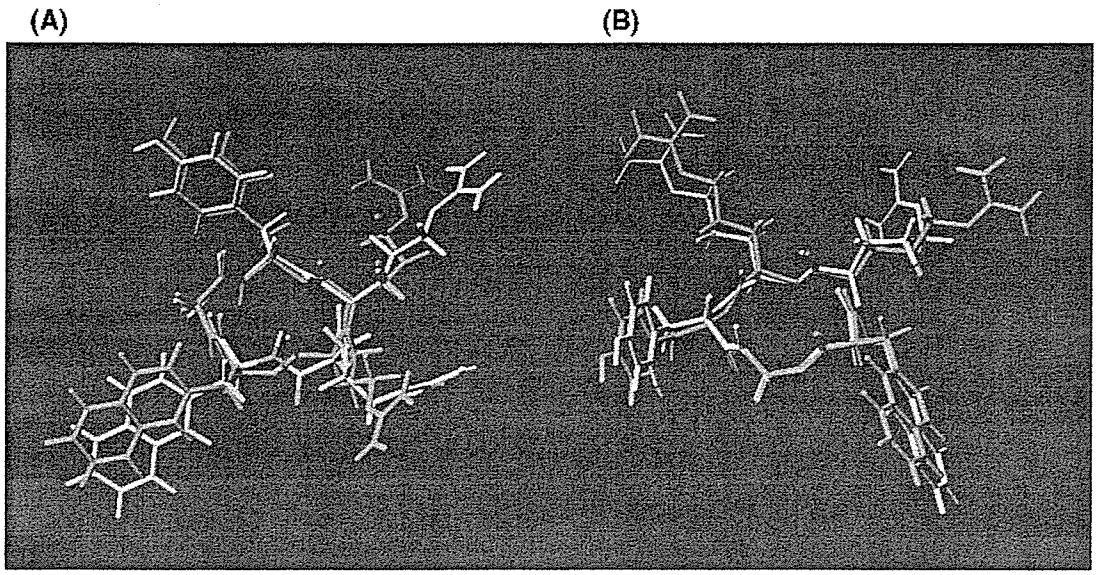

Figure 2. Superimpositions of low-energy structures of FC131 and **37a** (A) or **37c** (B). The FC131 structure is depicted in green, and the **37a** or **37c** structure is depicted in purple.

Conclusion

A set of (L-Arg-L/D-Nal)-type EADIs were synthesized from a single substrate of γ,δ-*cis*-γ,δ-epimino (*E*)-α,β-enoate by combination of MSA-mediated aziridinyl ring-opening reactions and *anti*-S_N2' reactions with organozinc−copper reagents that were prepared from 2-naphthylmethylZnBr and CuCN. Organozinc−copper-mediated α-alkylation reactions are thought to be useful for construction of several side chains at the α-position of EADIs, as organocopper-mediated α-alkylation reactions that have been generally used. Next, EADIs and RADIs of Arg-Nal and Nal-Gly, including the above EADIs, were synthesized and inserted into cyclic pentapeptides, FC131 analogues, to disclose biological importance of each amide bond. The present results will be useful for the development of nonpeptide CXCR4 antagonists derived from FC131. It is also noteworthy that EADI units were introduced into cyclic pentapeptides without any significant conformational changes in the pentagonal backbone structures, except for those of substituted (*E*)-alkene units, suggesting that the planar nature of (*E*)-alkene units caused the conformational maintenance of the backbones excluding the olefinic moiety. SA-MD analysis showed that the parent peptide (FC131) and the EADI-introduced pseudopeptides (**37a** and **37c**) have nearly equal distances between any two β-carbons in all of the side chains. It suggests that these compounds maintain similar dispositions of pharmacophores and that the biological differences between these compounds are derived from the (*E*)-alkene/amide bond units. As such, EADIs become useful tools for investigation of biological contributions of amide bonds.

Experimental Section

General. Melting points are uncorrected. ^{1}H NMR spectra were recorded using a JEOL EX-270, a JEOL AL-400, or a Bruker AM 600 spectrometer at 270, 400, or 600 MHz ^{1}H frequency in $CDCl_3$, respectively. Chemical shifts are reported in parts per million downfield from internal tetramethylsilane. Nominal (LRMS) and exact mass (HRMS) spectra were recorded on a JEOL JMS-01SG-2 or JMS-HX/HX 110A mass spectrometer. Ion-spray (IS)-mass spectrum was obtained with a Sciex API *IIIE* triple quadrupole mass spectrometer (Toronto, Canada). Optical rotations were measured in $CHCl_3$ or H_2O with a JASCO DIP-360 digital polarimeter (Tokyo, Japan) or a Horiba high-sensitive polarimeter SEPA-200 (Kyoto, Japan). For flash column chromatography, silica gel 60 H (silica gel for thin-layer chromatography, Merck) and Wakogel C-200 (silica gel for column chromatography) were employed. HPLC solvents were H_2O and MeCN, both containing 0.1% (v/v) TFA. For analytical HPLC, a Cosmosil 5C18-AR column (4.6 mm × 250 mm, Nacalai Tesque Inc., Kyoto, Japan) was eluted with a linear gradient of MeCN at a flow rate of 1 mL/min on a Waters model 600 (Nihon Millipore, Ltd., Tokyo, Japan). Preparative HPLC was performed on a Waters Delta Prep 4000 equipped with a Cosmosil 5C18-AR column (20 mm × 250 mm, Nacalai Tesque Inc.) using an isocratic mode of MeCN at a flow rate of 15 mL/min.

Boc-Arg(Mts)-OMe, 5. To a stirred solution of Boc-Arg(Mts)-OH (10.0 g, 21.9 mmol) in DMF (50 mL) at 4 °C were added potassium bicarbonate (4.39 g, 43.8 mmol) and methyl iodide (2.73 mL, 43.8 mmol), and the mixture was stirred at room temperature for 10 h. The reaction mixture was concentrated under reduced pressure. The residue was extracted with EtOAc, and the extract was washed successively with saturated citric acid, brine, saturated aqueous $NaHCO_3$, and brine and dried over $MgSO_4$. Concentration under reduced pressure gave 10.4 g (21.8 mmol, 100%) of methyl ester **5** as a yellow oil.

$[\alpha]^{22}_D$ −4.25 (*c* 0.47, $CHCl_3$). ^{1}H NMR (270 MHz, $CDCl_3$) δ: 1.42 (9H, s, *tert*-Bu), 1.61 (2H, br m, CH_2), 1.78 (2H, br m, CH_2), 2.59 (3H, s, Ar-*p*-Me), 2.66 (6H, s, Ar-*o*-Me), 3.22 (2H, br m, CH_2), 3.73 (3H, s, OMe), 4.21−4.28 (1H, m, CH), 5.23 (1H, d, J = 8.2 Hz, NH), 6.14 (3H, br, guanidino), 6.89 (2H, s, ArH). *m/z* (FAB-LRMS): 471 (MH^+), 415, 371, 289 (base peak), 119. Found (FAB-HRMS): 471.2268. Calcd for $C_{21}H_{35}O_6N_4S$ (MH^+): 471.2277.

***N*-*tert*-Butoxy-[2(*S*)-hydroxy-1(*S*)-[3-[[imino[[(2,4,6-trimethylphenyl)sulfonyl]amino]methyl]amino]propyl]but-3-enyl]formamide, 6.** To a stirred solution of Boc-Arg(Mts)-OMe, **5** (5.0 g, 10.6 mmol), in toluene/CH_2Cl_2 (1:1 (v/v) 100 mL) was added dropwise a solution of DIBAL-H in toluene (1.0 M, 32 mL, 32 mmol) at −50 °C under argon, and the mixture was stirred at −78 °C for 2 h. To the solution, was added dropwise a vinyl Grignard (CH_2=$CHMgCl$) reagent in THF (13 mL, 32 mmol) at −78 °C, and the mixture was stirred for 6 h with a gradual warming to 0 °C. The reaction was quenched with saturated aqueous citric acid at −78 °C, and organic solvents were concentrated under reduced pressure. The residue was extracted with EtOAc, and the extract was washed successively with saturated aqueous citric acid, satu-

rated aqueous $NaHCO_3$, and brine and dried over $MgSO_4$. Concentration under reduced pressure followed by flash column chromatography over silica gel with EtOAc/*n*-hexane (2:1) gave a *threo*-allyl alcohol **6** and an *erythro*-allyl alcohol (2*R* isomer of **6**) (12:1), in order of elution (**6**, 1.5 g, 30% yield from **5**).

Compound **6**: colorless oil. $[\alpha]^{22}_D$ −15.74 (*c* 0.63, $CHCl_3$). ^1H NMR (270 MHz, $CDCl_3$) δ: 1.40 (9H, s, *tert*-Bu), 1.57 (2H, br m, 2-CH_2), 1.70 (2H, br m, 1-CH_2), 2.26 (3H, s, Ar-*p*-Me), 2.66 (6H, s, Ar-*o*-Me), 3.24 (2H, br m, 3-CH_2), 3.55 (1H, br, 1-H), 4.08 (1H, br, 2-H), 4.97 (1H, d, J = 9.7 Hz, NH), 5.18 (1H, d, J = 10.5 Hz, C*H*H=), 5.28 (1H, d, J = 17.3 Hz, CH*H*=), 5.77−5.89 (1H, m, CH=), 6.20 (3H, br, guanidino), 6.89 (2H, s, ArH). *m/z* (ISMS): 469.5 (MH^+). Found (FAB-HRMS): 469.2490. Calcd for $C_{22}H_{37}O_5N_4S$ (MH^+): 469.2485.

Compound 2*R* isomer of **6**: colorless oil. $[\alpha]^{21}_D$ −4.57 (*c* 2.84, $CHCl_3$). ^1H NMR (270 MHz, $CDCl_3$) δ: 1.41 (9H, s, *tert*-Bu), 1.48 (2H, br m, 2-CH_2), 1.64 (2H, br m, 1-CH_2), 2.30 (3H, s, Ar-*p*-Me), 2.63 (6H, s, Ar-*o*-Me), 3.15 (2H, br m, 3-CH_2), 3.63 (1H, br, 1-H), 4.18 (1H, br, 2-H), 5.12 (1H, br, NH), 5.24 (1H, d, J = 10.5 Hz, CH*H*=), 5.32 (1H, d, J = 17.0 Hz, C*H*H=), 5.74−5.85 (1H, m, CH=), 6.32 (3H, br, guanidino), 6.95 (2H, s, ArH). *m/z* (ISMS): 469.5 (MH^+).

[2(*S*)-Hydroxy-1(*S*)-[3-[[imino[[(2,4,6-trimethylphenyl)-sulfonyl]amino]methyl]amino]propyl]but-3-enyl][(2-nitrophenyl)sulfonyl]amine, 7. To a mixture of allyl alcohol **6** (4.2 g, 9.0 mmol) and anisole (0.97 mL, 9.0 mmol) at 0 °C was added 4 M HCl/dioxane (100 mL), and the mixture was stirred at room temperature for 2 h. The mixture was concentrated under reduced pressure. To a stirred solution of the residue in $CHCl_3$ (20 mL) at 0 °C were added 2-nitrobenzenesulfonyl chloride (2.38 g, 10.8 mmol), triethylamine (Et_3N) (5 mL), and pyridine (20 mL), and the mixture was allowed to warm to room temperature, stirred at this temperature for 12 h, and extracted with $CHCl_3$. The extract was washed with saturated aqueous citric acid, saturated aqueous $NaHCO_3$, and brine and dried over $MgSO_4$. Concentration under reduced pressure followed by chromatography over silica gel with $CHCl_3$/MeOH (18:1) gave 3.2 g (5.8 mmol, 65% from **6**) of **7** as a yellow oil.

$[\alpha]^{23}_D$ −57.79 (*c* 1.83, $CHCl_3$). ^1H NMR (270 MHz, $CDCl_3$) δ: 1.61 (4H, br m, 1, 2-CH_2), 2.27 (3H, s, Ar-*p*-Me), 2.64 (6H, s, Ar-*o*-Me), 3.15 (2H, br m, 3-CH_2), 3.50 (1H, br, 1-H), 3.72−3.78 (1H, m, 2-H), 4.72 (1H, d, J = 10.5 Hz, C*H*H=), 5.07 (1H, d, J = 17.0 Hz, CH*H*=), 5.42−5.48 (1H, m, CH=), 5.90 (1H, d, J = 8.1 Hz, NH), 6.26 (3H, br, guanidino), 6.90 (2H, s, ArH), 7.65−7.69 (2H, m, ArH), 7.78−7.82 (1H, m, ArH), 8.04−8.08 (1H, m, ArH). *m/z* (ISMS): 554.5 (MH^+). Found (FAB-HRMS): 554.1735. Calcd for $C_{23}H_{32}O_7N_5S_2$ (MH^+): 554.1743.

3(*S*)-[3-[[Imino[(2,4,6-trimethylphenyl)sulfonyl]amino]methyl]amino]propyl]-1-[(2-nitrophenyl)sulfonyl]-2(*R*)-vinylaziridine, 8. To a stirred solution of allyl alcohol **7** (3.1 g, 5.6 mmol) in dry THF (30 mL) at 0 °C were added triphenylphosphine (1.6 g, 6.2 mmol) and diethyl azodicarbonate (2.4 mL of a 40% solution in toluene, 6.2 mmol), and the reaction mixture was stirred at this temperature for 30 min. The mixture was concentrated under reduced pressure and purified by chromatography over silica gel with EtOAc/*n*-hexane (2:1) to give 2.8 g (5.2 mmol, 93% yield from **7**) of aziridine **8** as a yellow oil.

$[\alpha]^{23}_D$ −10.45 (*c* 2.20, $CHCl_3$). ^1H NMR (270 MHz, $CDCl_3$) δ: 1.48 (4H, br m, 1, 2-CH_2), 2.26 (3H, s, Ar-*p*-Me), 2.65 (6H, s, Ar-*o*-Me), 3.02 (1H, br, 2-H), 3.15 (2H, br m, 3-CH_2), 3.46 (1H, br, 3-H), 5.29 (1H, d, J = 9.7 Hz, C*H*H=), 5.42 (1H, d, J = 17.0 Hz, CH*H*=), 5.45−5.53 (1H, m, CH=), 6.41 (3H, br, guanidino), 6.88 (2H, s, ArH), 7.45−7.50 (2H, m, ArH), 7.54−7.75 (2H, m, ArH). *m/z* (ISMS): 536.5 (MH^+). Found (FAB-HRMS): 536.1630. Calcd for $C_{23}H_{30}O_6N_5S_2$ (MH^+): 536.1638.

Phenylmethyl 3-3(*S*)-[3-[[Imino[(2, 4, 6-trimethylphenyl)sulfonyl]amino]methyl]amino]propyl]-2(*R*)-[(2-nitrophenyl)sulfonyl-2-aziridinyl]prop-2-enoate, 9. To a solution of aziridine **8** (1.2 g, 2.2 mmol) in CH_2Cl_2 (30 mL) was bubbled O_3 gas at −78 °C until a blue color persisted. To the above solution was added Me_2S (1.7 mL, 22 mmol), and the mixture was stirred for 30 min and then dried over $MgSO_4$. Concentration under reduced pressure gave an oily residue of a crude aldehyde, which was used immediately in the next step without further purification. To a stirred suspension of LiCl (230 mg, 5.4 mmol) in MeCN (5 mL) under argon, were added $(EtO)_2P(O)CH_2CO_2Bn$ (1.5 mL, 5.4 mmol) and $(^iPr)_2NEt$ (DIPEA) (0.94 mL, 5.4 mmol) at 0 °C. After 20 min, the above aldehyde in MeCN (15 mL) was added to the mixture at 0 °C, and the mixture was stirred at this temperature for 8 h. The mixture was concentrated under reduced pressure, and the residue was extracted with EtOAc. The extract was washed successively with saturated aqueous citric acid and H_2O and dried over $MgSO_4$. Concentration under reduced pressure followed by chromatography over silica gel with $CHCl_3$/MeOH (40:1) gave the title compound **9** (1.0 g, 1.5 mmol, 67% yield from **8**) as a colorless oil.

$[\alpha]^{23}_D$ −10.1 (*c* 1.49, $CHCl_3$). ^1H NMR (270 MHz, $CDCl_3$) δ: 1.63 (4H, br m, 1, 2-CH_2), 2.17 (3H, s, Ar-*p*-Me), 2.64 (6H, s, Ar-*o*-Me), 3.20 (2H, br m, 3-CH_2), 3.22 (1H, br, 2-H), 3.61 (1H, br, 3-H), 5.15 (2H, s, CH_2), 6.18 (1H, dd, J = 15.7, 0.8 Hz, CH=), 6.22 (3H, br, guanidino), 6.66 (1H, dd, J = 15.5, 6.9 Hz, CH=), 6.88 (2H, s, ArH), 7.34 (5H, s, ArH), 7.56−7.60 (1H, m, ArH), 7.71−7.79 (2H, m, ArH), 8.13−8.17 (1H, m, ArH). *m/z* (ISMS): 670.5 (MH^+). Found (FAB-HRMS): 670.2019. Calcd for $C_{31}H_{36}O_8N_5S_2$ (MH^+): 670.2005.

Phenylmethyl 8-[[Imino[(2,4,6-trimethylphenyl)sulfonyl]amino]methyl]amino]-5(*S*)-[[(2-nitrophenyl)sulfonyl]amino]-2(*R*)-(naphthylmethyl)oct-3-enoate [Ns-L-Arg-(Mts)-ψ[(*E*)-CH=CH]-L-Nal-OBn], 10. To a stirred solution of CuCN (219 mg, 2.45 mmol) and LiCl (207 mg, 4.89 mmol) in dry THF (3.0 mL) under argon at −78 °C, was added dropwise 0.5 M (2-naphthylmethyl)zincbromide in THF solution (4.9 mL, 2.45 mmol), and the mixture was stirred at 0 °C for 10 min. A solution of enoate **9** (273 mg, 0.408 mmol) in dry THF (9.0 mL) was added dropwise to the above mixture at −78 °C with stirring, and the stirring was continued for 30 min followed by quenching with 10 mL of a 1:1 saturated aqueous NH_4Cl/28% NH_4OH solution. The mixture was extracted with Et_2O, and the extract was washed with saturated aqueous NH_4Cl and brine and dried over $MgSO_4$. Concentration under reduced pressure gave an oily residue, which was purified by chromatography over silica gel with *n*-hexane/EtOAc (1:2) to yield 273 mg (0.337 mmol, 83% yield from **9**) of compound **10** as a yellow oil. $[\alpha]^{33}_D$ −80.9 (*c* 0.61, $CHCl_3$). ^1H NMR (270 MHz, $CDCl_3$) δ: 1.35 (2H, br m, 2-CH_2), 1.55 (2H, br m, 1-CH_2), 2.04 (3H, s, Ar-*p*-Me), 2.26 (6H, s, Ar-*o*-Me), 2.97 (2H, br, CH_2), 2.98 (2H, br m, 3-CH_2), 3.20−3.25 (1H, m, 2-H), 3.90 (1H, br, 5-H), 4.93 (2H, s, CH_2), 5.24 (1H, dd, J = 15.5, 6.9 Hz, CH=), 5.50 (1H, dd, J = 15.4, 8.4 Hz, CH=), 5.67 (1H, d, J = 4.6 Hz, NH), 5.95 (3H, br, guanidino), 6.89 (2H, s, ArH), 7.05−7.28 (7H, m, ArH), 7.42−7.77 (9H, m, ArH), 7.96−8.00 (1H, m, ArH). *m/z* (ISMS): 814.0 (MH^+). Found (FAB-HRMS): 812.2803. Calcd for $C_{42}H_{46}O_8N_5S_2$ (MH^+): 812.2788.

Phenylmethyl 5(*S*)-[(Fluoren-9-ylmethoxy)carbonyl-amino]-8-[[imino[[(2,4,6-trimethylphenyl)sulfonyl]amino]methyl]amino]-2(*R*)-(2-naphthylmethyl)oct-3-enoate [Fmoc-L-Arg(Mts)-ψ[(*E*)-CH=CH]-L-Nal-OBn], 11. To a stirred solution of enoate **10** (81 mg, 0.10 mmol) in DMSO/MeCN (1:49, 5 mL), were added thiophenol (31 μL, 0.3 mmol) and K_2CO_3 (55 mg, 0.4 mmol) at room temperature, and the mixture was stirred at 50 °C for 1 h. The solution was filtered, and the filtrate was concentrated under reduced pressure. The residue was extracted with EtOAc, washed with brine, and dried over $MgSO_4$. Concentration under reduced pressure gave an oily residue, which was dissolved in THF/H_2O (1:1, 50 mL). Fmoc-OSu (33 mg, 0.1 mmol) and Et_3N (27 μL, 0.19 mmol) were added to the above solution at 0 °C. After being stirred for 6 h, the mixture was acidified with 0.1 M HCl and then extracted with EtOAc. The extract was washed with 0.1 M HCl and brine and dried over $MgSO_4$. Concentration under reduced pressure followed by chromatography over silica gel with *n*-hexane/EtOAc (1:2) gave the title compound **11** (60 mg, 70.9 μmol, 71% yield from **10**) as a colorless oil.

$[\alpha]^{29}_D$ −11.2 (*c* 0.63, $CHCl_3$). ^1H NMR (270 MHz, $CDCl_3$) δ: 1.26 (4H, br m, 1, 2-CH_2), 2.18 (3H, s, Ar-*p*-Me), 2.63 (6H, s,

Ar-*o*-Me), 2.94 (2H, br, CH_2), 3.19 (2H, br m, 3-CH_2), 3.38 (1H, br, 2-H), 3.96 (1H, br, 5-H), 4.12 (1H, t, J = 5.8 Hz, ArH), 4.35 (2H, t, J = 5.94 Hz, CH_2), 4.82 (1H, br, NH), 5.01 (2H, s, CH_2), 5.24 (1H, dd, J = 15.0, 5.7 Hz, CH=), 5.64 (1H, dd, J = 14.4, 7.8 Hz, CH=), 6.16 (3H, br, guanidino), 6.81 (2H, s, ArH), 7.08–7.28 (8H, m, ArH), 7.33–7.42 (4H, m, ArH), 7.42–7.54 (3H, m, ArH), 7.64–7.74 (5H, m, ArH). *m/z* (ISMS): 850.0 (MH^+). Found (FAB-HRMS): 849.3664. Calcd for $C_{51}H_{53}O_6N_4S_2$ (MH^+): 849.3686.

5(*S*)-[(Fluoren-9-ylmethoxy)carbonylamino]-8-[[imino-[[(2, 4, 6-trimethylphenyl)sulfonyl]amino]methyl]amino]-2(*R*)-(2-naphthylmethyl)oct-3-enoic Acid [Fmoc-L-Arg-(Mts)-ψ[(*E*)-CH=CH]-L-Nal-OH], 12. The enoate **11** (30 mg, 0.037 mmol) was dissolved in TFA (10 mL), and thioanisole (500 μL), *m*-cresol (200 μL), and 1,2-ethanedithiol (100 μL) were added to the solution at 0 °C, and the mixture was stirred for 12 h at room temperature. The mixture was concentrated under reduced pressure and extracted with EtOAc. The extract was washed with brine and dried over $MgSO_4$. Concentration under reduced pressure followed by chromatography over silica gel with *n*-hexane/EtOAc (1:4) gave the title compound **12** (28 mg, 0.036 mmol, 98% yield from **11**) as a colorless oil.

$[\alpha]^{23}_D$ −15.2 (*c* 0.07, $CHCl_3$). ^1H NMR (600 MHz, $CDCl_3$) δ: 1.25 (4H, br m, 1, 2-CH_2), 2.20 (3H, s, Ar-*p*-Me), 2.62 (6H, s, Ar-*o*-Me), 2.86 (2H, br, CH_2), 3.05 (2H, br m, 3-CH_2), 3.49 (1H, br, 2-H), 3.68 (1H, br, 5-H), 4.10 (1H, br, ArH), 4.20–4.26 (2H, m, CH_2), 4.93 (1H, br, CH=), 5.34 (1H, br, CH=), 5.38 (1H, br, NH), 5.95 (3H, br, guanidino), 6.84 (2H, s, ArH), 7.20–7.41 (7H, m, ArH), 7.48–7.57 (3H, m, ArH), 7.65–7.77 (5H, m, ArH). *m/z* (ISMS): 760.0 (MH^+). Found (FAB-HRMS): 759.3228. Calcd for $C_{44}H_{47}O_6N_4S_2$ (MH^+): 759.3216.

Phenylmethyl 8-[[Imino[[(2, 4, 6-trimethylphenyl)sulfonyl]amino]methyl]amino]-5(*S*)-[[(2-nitrophenyl)-sulfonyl]amino]-2(*S*)-(naphthylmethyl)oct-3-enoate [Ns-L-Arg(Mts)-ψ[(*E*)-CH=CH]-D-Nal-OBn], 14. To a stirred solution of enoate **9** (500 mg, 0.75 mmol) in $CHCl_3$ (5 mL) was added dropwise MSA (435 μL, 6.7 mmol) at room temperature with stirring, and the stirring was continued for 20 min. The mixture was extracted with EtOAc, and the extract was washed successively with aqueous 5% citric acid, water, aqueous 5% $NaHCO_3$, and water and dried over $MgSO_4$. Concentration under reduced pressure gave an oily residue of the crude mesylate **13**, which was used directly in the following step without further purification. To a stirred slurry of CuCN (269 mg, 3.0 mmol) in dry THF (5 mL) under argon at −78 °C was added dropwise (2-naphthylmethyl)zincbromide in THF solution (6.0 mL, 3.0 mmol), and the mixture was stirred at 0 °C for 15 min followed by addition of $BF_3 \cdot Et_2O$ (369 μL, 3.0 mmol) at −78 °C and then stirred at −78 °C for 15 min. To the mixture at −78 °C with stirring was added by syringe a solution of the crude mesylate **13** in THF (10 mL), and the stirring was continued at −78 °C for 1 h followed by quenching with saturated aqueous NH_4Cl and aqueous 28% NH_4OH (1:1) at 0 °C. The mixture was allowed to warm to room temperature and extracted with Et_2O. The extract was washed with H_2O, dried over $MgSO_4$, and concentrated under reduced pressure. The residue was purified by chromatography over silica gel with *n*-hexane/EtOAc (1:2) to give 408 mg (0.50 mmol, 67% from **9**) of protected EADI **14** as a yellow oil. $[\alpha]^{32}_D$ −41.7 (*c* 0.60, $CHCl_3$). ^1H NMR (270 MHz, $CDCl_3$) δ: 1.54 (4H, br m, 1, 2-CH_2), 2.25 (3H, s, Ar-*p*-Me), 2.66 (6H, s, Ar-*o*-Me), 2.86 (2H, br m, 3-CH_2), 2.98–3.06 (2H, m, CH_2), 3.15–3.23 (1H, m, 2-H), 3.78–3.88 (1H, m, 5-H), 4.98 (2H, s, CH_2), 5.09 (1H, dd, J = 15.5, 8.0 Hz, CH=), 5.49 (1H, dd, J = 15.5, 8.2 Hz, CH=), 5.57 (1H, d, J = 8.4 Hz, NH), 6.09 (3H, br, guanidino), 6.89 (2H, s, ArH), 7.10–7.26 (7H, m, ArH), 7.37–7.76 (9H, m, ArH), 7.95–7.98 (1H, m, ArH). *m/z* (ISMS): 814.0 (MH^+). Found (FAB-HRMS): 812.2775. Calcd for $C_{42}H_{46}O_8N_5S_2$ (MH^+): 812.2788.

Phenylmethyl 5(*S*)-[(Fluoren-9-ylmethoxy)carbonyl-amino]-8-[[imino[[(2,4,6-trimethylphenyl)sulfonyl]ami-no]methyl]amino]-2(*S*)-(2-naphthylmethyl)oct-3-enoate [Fmoc-L-Arg(Mts)-ψ[(*E*)-CH=CH]-D-Nal-OBn], 15. By use of a procedure identical with that described for the preparation of **11** from **10**, the enoate **14** (30 mg, 37 μmol) was converted into 28 mg (36 μmol, 98% yield from **14**) of the title compound **15** as a colorless oil.

$[\alpha]^{29}_D$ −1.6 (*c* 0.61, $CHCl_3$). ^1H NMR (270 MHz, $CDCl_3$) δ: 1.14–1.30 (4H, br m, 1, 2-CH_2), 2.17 (3H, s, Ar-*p*-Me), 2.62 (6H, s, Ar-*o*-Me), 2.91 (2H, br m, 3-CH_2), 3.15–3.23 (2H, m, CH_2), 3.40 (1H, br, 2-H), 3.95 (1H, br, 5-H), 4.11 (1H, t, J = 6.5 Hz, ArH), 4.33 (2H, d, J = 5.7 Hz, CH_2), 4.85 (1H, d, J = 6.8 Hz, NH), 5.00 (2H, s, CH_2), 5.25 (1H, dd, J = 16.7, 6.8 Hz, CH=), 5.61 (1H, dd, J = 14.3, 7.6 Hz, CH=), 6.13 (3H, br, guanidino), 6.81 (2H, s, ArH), 7.09–7.27 (8H, m, ArH), 7.32–7.45 (4H, m, ArH), 7.46–7.56 (3H, m, ArH), 7.64–7.73 (5H, m, ArH). *m/z* (ISMS): 850.0 (MH^+). Found (FAB-HRMS): 849.3698. Calcd for $C_{51}H_{53}O_6N_4S_2$ (MH^+): 849.3686.

5(*S*)-[(Fluoren-9-ylmethoxy)carbonylamino]-8-[[imino-[[(2, 4, 6-trimethylphenyl)sulfonyl]amino]methyl]amino]-2(*S*)-(2-naphthylmethyl)oct-3-enoic Acid [Fmoc-L-Arg-(Mts)-ψ[(*E*)-CH=CH]-D-Nal-OH], 16. By use of a procedure identical with that described for the preparation of **12** from **11**, the enoate **15** (153 mg, 0.19 mmol) was converted into 144 mg (0.19 mmol, 99% yield from **15**) of the title compound **16** as a colorless oil.

$[\alpha]^{23}_D$ 10.8 (*c* 0.19, $CHCl_3$). ^1H NMR (270 MHz, $CDCl_3$) δ: 1.24 (4H, br m, 1, 2-CH_2), 2.17 (3H, s, Ar-*p*-Me), 2.70 (6H, s, Ar-*o*-Me), 2.90 (2H, br m, 3-CH_2), 3.07 (2H, m, CH_2), 3.29 (1H, br, 2-H), 3.67 (1H, br, 5-H), 4.06 (1H, t, J = 8.2 Hz, ArH), 4.28 (2H, d, J = 5.9 Hz, CH_2), 5.12 (1H, d, J = 5.9 Hz, NH), 5.26 (1H, dd, J = 15.0, 5.8 Hz, CH=), 5.59 (1H, dd, J = 15.0, 8.0 Hz, CH=), 6.19 (3H, br, guanidino), 6.80 (2H, s, ArH), 7.18–7.40 (7H, m, ArH), 7.46–7.54 (3H, m, ArH), 7.59–7.70 (5H, m, ArH). *m/z* (ISMS): 760.0 (MH^+). Found (FAB-HRMS): 759.3201. Calcd for $C_{44}H_{47}O_6N_4S_2$ (MH^+): 759.3216.

H-D-Tyr(O^{t}Bu)-Arg(Pbf)-Arg(Mts)-ψ[(*E*)-CH=CH]-Nal-Gly-NHNHCO−Wang Resin. *p*-Nitrophenyl carbonate Wang resin **33** (Calbiochem-Novabiochem Japan, Ltd., Tokyo, Japan, 0.93 mmol/g, 323 mg, 0.3 mmol) was treated with $NH_2NH_2 \cdot H_2O$ (146 μL, 3.0 mmol) in DMF (3 mL) at room temperature for 2 h to give a hydrazide linker **34**. Protected peptide−resins were manually constructed by Fmoc-based solid-phase peptide synthesis. ^{t}Bu for Tyr and Mts or Pbf for Arg were employed for side-chain protection. Fmoc deprotection was achieved by 20% piperidine in DMF (1 min × 2 and 15 min × 1). Fmoc−amino acids including EADIs or RADIs were condensed to free amino groups by treatment with 3 equiv of reagents (Fmoc−amino acid, *N,N'*-diisopropylcarbodiimide (DIPCDI) and HOBt·H_2O) in DMF for 1.5 h.

***cyclo*(-D-Tyr-Arg-Arg-ψ[(*E*)-CH=CH]-Nal-Gly-)·2TFA (37a).** The protected **37a** resin (34 mg, 0.025 mmol) was treated with TFA (0.5 mL) in $CHCl_3$ (4.5 mL) at room temperature for 2 h, and the mixture was filtered. Concentration of the filtrate under reduced pressure gave a crude hydrazide (H-D-Tyr-Arg(Pbf)-Arg(Mts)-ψ[(*E*)-CH=CH]-Nal-Gly-$NHNH_2$) as a colorless powder. To a stirred solution of the hydrazide in DMF (1 mL) were added a solution of 4 M HCl in DMF (16.6 μL, 75 μmol) and isoamyl nitrite (40 μL, 0.20 mmol) at −30 °C. After being stirred at −10 °C for 20 min, the mixture was diluted with precooled DMF (50 mL). To the above solution was added DIPEA (191 μL, 1.1 mmol) at −30 °C, and the mixture was stirred for 48 h at −20 °C. Concentration under reduced pressure gave a yellow oil (crude *cyclo*(-D-Tyr-Arg(Pbf)-Arg(Mts)-ψ[(*E*)-CH=CH]-Nal-Gly-)). To the protected cyclic peptide were added *m*-cresol (0.4 mL, 3.6 mmol), 1, 2-ethanedithiol (160 μL, 1.9 mmol), thioanisole (1.0 mL, 8.5 mmol), TFA (10 mL), and bromotrimethylsilane (1.2 mL, 9.1 mmol) at 0 °C, and the stirring was continued at room temperature for 12 h. Concentration under reduced pressure and purification by preparative HPLC gave the cyclic pseudopeptide **37a** (8.5 mg, 36% yield from protected **37a** resin) as a freeze-dried powder.

$[\alpha]^{27}_D$ −53.3 (*c* 0.24, H_2O). t_R = 28.6 min (linear gradient of MeCN in H_2O, 10 to 40% over 30 min). *m/z* (ISMS): 714.0 (MH^+). Found (FAB-HRMS): 713.3879. Calcd for $C_{37}H_{49}O_5N_{10}$ (MH^+): 713.3887.

***cyclo*(-D-Tyr-Arg-Arg-ψ[(*E*)-CH=CH]-D-Nal-Gly-)·2TFA (37f).** By use of a procedure identical with that described

for the preparation of **37a**, the protected **37f** (34 mg, 0.025 mmol) was converted into 9.8 mg (10.5 μmol, 42%) of the title compound **37f**, as a freeze-dried powder.

$[\alpha]^{26}_D$ −32.0 (*c* 0.13, H_2O). t_R = 28.9 min (linear gradient of MeCN in H_2O, 10 to 40% over 30 min). *m/z* (ISMS): 714.0 (MH^+). Found (FAB-HRMS): 713.3903. Calcd for $C_{37}H_{49}O_5N_{10}$ (MH^+): 713.3887.

***(tert*-Butoxy)-*N*-[2(*R,S*)-hydroxy-1(*S*)-(2-naphthylmethyl)but-3-enyl]formamide, 20.** To a stirred solution of Boc-Nal-OMe **19** (4.0 g, 12.2 mmol) in CH_2Cl_2 (100 mL) was added dropwise a solution of DIBAL-H in toluene (1.0 M, 24.4 mL, 24.4 mmol) at −78 °C under argon, and the mixture was stirred at −78 °C for 2 h. To the solution was added dropwise a vinyl Grignard (CH_2=CHMgCl) reagent in THF (12.6 mL, 36.6 mmol) at −78 °C, and the mixture was stirred for 6 h with warming to 0 °C. The reaction was quenched with saturated aqueous citric acid at −78 °C, and organic solvents were concentrated under reduced pressure. The residue was extracted with EtOAc, and the extract was washed successively with saturated aqueous citric acid, saturated aqueous $NaHCO_3$, and brine and dried over $MgSO_4$. Concentration under reduced pressure followed by chromatography over silica gel with EtOAc/*n*-hexane (3:1) gave a mixture of *threo*- and *erythro*-allyl alcohols **20** (1.4 g, 35% yield from **19**) as a colorless oil. The mixture of diastereoisomer was used in the following step without further purification.

^1H NMR (270 MHz, $CDCl_3$) δ: 1.24−1.36 (9H, br, *tert*-Bu), 2.90−2.94 (1H, br, 2-H), 3.00−3.03 (2H, br, CH_2), 3.86−3.94 (1H, br, 1-H), 4.95−5.01 (1H, br, NH), 5.13−5.17 (1H, m, C*H*H=), 5.22−5.29 (1H, m, CH*H*=), 5.82−5.94 (1H, m, CH=), 7.38−7.43 (3H, m, ArH), 7.68−7.80 (4H, m, ArH). *m/z* (ISMS): 328.5 (MH^+). Found (FAB-HRMS): 328.1921. Calcd for $C_{20}H_{26}O_3N$ (MH^+): 328.1913.

1(*S*)-[1-[(*tert*-Butoxy)carbonylamino]-2-(naphthyl)ethyl]prop-2(*R, S*)-enyl Acetate, 21. To a stirred solution of allyl alcohol **20** (8.5 g, 26.0 mmol) in $CHCl_3$ (10 mL), were added acetic anhydride (11.0 mL, 117 mmol) and pyridine (18.9 mL, 234 mmol) at 4 °C, and the mixture was stirred at room temperature for 6 h. The mixture was concentrated under reduced pressure. The residue was extracted with EtOAc, and the extract was washed with aqueous 5% $NaHCO_3$, aqueous 1 M HCl, and brine and dried over $MgSO_4$. Concentration under reduced pressure followed by chromatography over silica gel with EtOAc/*n*-hexane (2:1) gave acetates **21** (5.7 g, 59% yield from **20**) as a colorless oil.

^1H NMR (270 MHz, $CDCl_3$) δ: 1.29−1.37 (9H, br, *tert*-Bu), 2.06−2.08 (3H, br, Me), 2.80−2.84 (1H, br, 2-H), 2.89−2.95 (2H, br, CH_2), 4.14−4.20 (1H, br, 1-H), 4.74−4.78 (1H, br, NH), 5.20−5.24 (1H, br m, C*H*H=), 5.25−5.30 (1H, br m, CH*H*=), 5.74−5.80 (1H, m, CH=), 7.30−7.42 (3H, m, ArH), 7.60−7.76 (4H, m, ArH). *m/z* (ISMS): 370.5 (MH^+). Found (FAB-HRMS): 370.2016. Calcd for $C_{22}H_{28}O_4N$ (MH^+): 370.2018.

***tert*-Butyl 4(*R,S*)-Acetoxy-5(*S*)-[(*tert*-butoxy)carbonylamino]-6-(2-naphthyl)hex-2-enoate, 22.** To a solution of acetate **21** (5.7 g, 15.4 mmol) in CH_2Cl_2 (40 mL) was bubbled O_3 gas at −78 °C until a blue color persisted. To the above solution, was added Me_2S (11 mL, 154 mmol), and the mixture was stirred for 30 min. The mixture was dried over $MgSO_4$. Concentration under reduced pressure gave an oily residue of a crude aldehyde, which was used immediately in the next step without further purification. To a stirred suspension of LiCl (1.57 g, 37 mmol) in MeCN (10 mL) under argon were added $(EtO)_2P(O)CH_2CO_2{}^tBu$ (8.7 mL, 37 mmol) and DIPEA (6.4 mL, 37 mmol) at 0 °C. After 20 min, the above aldehyde in MeCN (20 mL) was added to the above mixture at 0 °C, and the mixture was stirred at this temperature for 8 h. The mixture was concentrated under reduced pressure, and the residue was extracted with EtOAc. The extract was washed successively with saturated aqueous citric acid and H_2O and dried over $MgSO_4$. Concentration under reduced pressure followed by chromatography over silica gel with EtOAc/*n*-hexane (1:2) gave enoates **22** (2.1 g, 29% yield from **21**) as a white amorphous semisolid.

Found: C, 68.97; H, 7.60; N, 2.92. $C_{27}H_{35}O_6N$ Calcd: C, 69.06; H, 7.51; N, 2.98. ^1H NMR (270 MHz, $CDCl_3$) δ: 1.34−1.38 (9H, br, *tert*-Bu), 1.43−1.47 (9H, br, *tert*-Bu), 2.13−2.17 (3H, br, Me), 2.91−2.99 (2H, br, CH_2), 4.22−4.32 (1H, br, 5-H), 4.71−4.77 (1H, br, 4-H), 5.42−5.46 (1H, br, NH), 5.79−5.99 (1H, m, CH=), 6.70−6.83 (1H, m, CH=), 7.43−7.49 (3H, m, ArH), 7.77−7.82 (4H, m, Ar). *m/z* (FAB-LRMS): 468 [(M−H)$^-$], 305, 199, 153, 151, and 46 (base peak). Found (FAB-HRMS): 468.2375. Calcd for $C_{27}H_{34}O_6N$ [(M−H)$^-$]: 468.2386.

***tert*-Butyl 5(*S*)-[(*tert*-Butoxy)carbonylamino]-6-(2-naphthyl)hex-3-enoate (Boc-L-Nal=Gly-O^{t}Bu), 23.** To a stirred slurry of Sm (900 mg, 6.0 mmol) in dry THF (20 mL) under argon at room temperature was added a solution of CH_2I_2 (322 μL, 4.0 mmol) in dry THF (20 mL), and the slurry was stirred at room temperature for 2 h until a dark green color persisted. To a stirred solution of enoate **22** (600 mg, 1.3 mmol) in dry THF (16 mL) in the other vessel were added *tert*-BuOH (8 mL, excess) and the above SmI_2 solution (38 mL, 3.8 mmol) under argon at room temperature, and the mixture was stirred for 1 h. The reaction was then quenched with saturated aqueous NH_4Cl (10 mL) at 4 °C, and the mixture was extracted with Et_2O (20 mL). The extract was washed with saturated aqueous NH_4Cl and brine and dried over $MgSO_4$. Concentration under reduced pressure followed by chromatography over silica gel with EtOAc/*n*-hexane (1:4) gave the enoate **23** (530 mg, 95% yield from **22**) as white crystals.

Mp: 80−82 °C (from *n*-hexane). Found: C, 73.17; H, 8.17; N, 3.39. $C_{25}H_{33}O_4N$ Calcd: C, 72.96; H, 8.08; N, 3.40. $[\alpha]^{25}_D$ 11.00 (*c* 1.09, $CHCl_3$). ^1H NMR (400 MHz, $CDCl_3$) δ: 1.37 (9H, s, *tert*-Bu), 1.41 (9H, s, *tert*-Bu), 2.93 (2H, d, *J* = 6.4 Hz, 6-CH_2), 2.98 (2H, d, *J* = 6.8 Hz, 2-CH_2), 4.48−4.59 (1H, br, NH), 5.43 (1H, t, *J* = 11.2 Hz, 5-H), 5.55 (1H, dd, *J* = 15.6, 5.6 Hz, CH=), 5.61−5.69 (1H, br, CH=), 7.31−7.46 (3H, m, ArH), 7.60−7.62 (1H, br, ArH), 7.74−7.78 (3H, m, ArH). *m/z* (ISMS): 412.0 (MH^+). Found (FAB-HRMS): 412.2491. Calcd for $C_{25}H_{34}O_4N$ (MH^+): 412.5418.

5(*S*)-[(Fluoren-9-ylmethoxy)carbonylamino]-6-(2-naphthyl)hex-3-enoic Acid (Fmoc-L-Nal=Gly-OH), 24. The enoate **23** (1.79 g, 4.35 mmol) was dissolved in TFA (30 mL), anisole (472 μL, 4.35 mmol) was added to the solution at 4 °C, and the mixture was stirred at room temperature for 2 h. The mixture was concentrated under reduced pressure and dissolved in THF and H_2O (1:1 (v/v) 20 mL). To the stirred solution were added Fmoc-OSu (1.47 g, 4.35 mmol) and Et_3N (10 mL, 71.7 mmol) at 4 °C, and the mixture was stirred at room temperature for 8 h. The mixture was acidified with aqueous 1 M HCl and was extracted with EtOAc. The extract was washed with aqueous 0.1 M HCl and brine and dried over $MgSO_4$. Concentration under reduced pressure followed by chromatography over silica gel with EtOAc/*n*-hexane (3:1) gave the enoic acid **24** (1.61 g, 78% yield from **23**) as white crystals.

Mp: 134−136 °C (from *n*-hexane). $[\alpha]^{23}_D$ −2.75 (*c* 0.73, $CHCl_3$). ^1H NMR (400 MHz, $CDCl_3$) δ: 2.96 (2H, br, 6-CH_2), 3.03 (2H, br, 2-CH_2), 4.14 (1H, t, *J* = 6.6 Hz, ArH), 4.32 (1H, dd, *J* = 14.9, 7.2 Hz, CH=), 4.38 (1H, m, CH=) 4.54 (1H, d, *J* = 7.6 Hz, CH_2), 4.81 (1H, br, 5-H), 5.62 (1H, br, NH), 7.18−7.28 (2H, m, ArH), 7.30−7.52 (5H, m, ArH), 7.57−7.63 (2H, m, ArH), 7.70−7.79 (6H, m, ArH). *m/z* (ISMS): 478.0 (MH^+). Found (FAB-HRMS): 478.2016. Calcd for $C_{31}H_{28}O_4N$ (MH^+): 478.2018.

H-D-Tyr(O^{t}Bu)-Arg(Pbf)-Arg(Pbf)-Nal-ψ[(*E*)-CH=CH]-Gly-NHNHCO−Wang Resin. On the hydrazide resin, were coupled successively Fmoc-D-Tyr(O^{t}Bu)-OH, Fmoc-Nal-ψ[(*E*)-CH=CH]-Gly-OH, and Fmoc-Arg(Pbf)-OH by use of the procedure identical with that described for the preparation of H-D-Tyr(O^{t}Bu)-Arg(Pbf)-Arg(Mts)-ψ[(*E*)-CH=CH]-Nal-Gly-NHNHCO−Wang resin to afford the protected **37c** resin.

***cyclo*(-D-Tyr-Arg-Arg-Nal-ψ[(*E*)-CH=CH]-Gly-)·2TFA (37c).** By use of a procedure identical with that described for the preparation of **37a**, the protected **37c** resin (173 mg, 0.13 mmol) was converted into 7.0 mg (7.4 μmol, 5.9%) of the title compound **37c**, as a freeze-dried powder.

$[\alpha]^{21}_D$ −43.1 (*c* 0.33, H_2O). t_R = 24.3 min (linear gradient of MeCN in H_2O, 10 to 40% over 30 min). *m/z* (ISMS): 713.0